



Cite this: *Mater. Adv.*, 2024,  
5, 453

## Porous nanomaterials for biosensing and related biological application in *in vitro/vivo* usability

Shaojun Liu,<sup>ab</sup> Xiaoxiao He,<sup>ab</sup> Xi Hu,<sup>ab</sup> Yaoyang Pu<sup>ab</sup> and Xiang Mao  <sup>ab</sup>

Porous nanomaterials (PNMs) refer to materials that have a porous structure on the nanoscale, characterized by a network of interconnected pores or voids. These materials exhibit unique physical and chemical properties due to their nanoscale size and the presence of pores. With the continuous development in nanotechnology and materials science, significant advancements have been realized in the design and approaches for various applications. In this case, PNMs have attracted significant attention due to their excellent biocompatibility, high loading capacity, controllable designability, and advantages in optical imaging. Therefore, it is necessary to investigate the ongoing developments in porous structures, particularly their applications in biosensing and *in vivo* scenarios, to demonstrate the advancements and latest research trends in this field. In this review, we present the diverse applications of PNMs, including porous silicon structures with facile approaches and expandable physical or optical properties, resulting in an excellent bioimaging performance; as useful substrates with superior loading capacity and easy intracellularization for drug delivery; and their good biocompatibility, degradability, and flexibility, making them suitable for *in vivo* applications, which can be achieved through a self-assembly path. Furthermore, the constituents of PNMs are highlighted and the influence of different factors on their *in vivo* and *in vitro* (biocompatibility and cytotoxicity) characteristics demonstrated. All these characteristics are appropriate for *in vivo* applications, outlining the significant potential of PNMs for biological applications and biosensing. The results show that PNMs are viable alternatives in current research and clinical applications. In this review, each section discusses and summarizes representative examples and analyzes the use of PNMs in biomedicine. Finally, the future of PNMs in biomedicine is explored, which can help researchers in understanding their prospective development.

Received 3rd August 2023,  
Accepted 18th December 2023

DOI: 10.1039/d3ma00498h

[rsc.li/materials-advances](http://rsc.li/materials-advances)

## 1. Introduction

In recent decades, encouraging progress has been realized in the biological applications of porous nanomaterials (PNMs).<sup>1,2</sup> PNMs are materials with tunable pore sizes and specific pore structures. Nanoporous silica, nanometallic organic frameworks (MOFs), nanoporous polymeric membranes, and nanoporous metals are typical porous nanomaterials.<sup>3–6</sup> PNMs exhibit high design flexibility, enabling their properties to be tuned through surface modification or alterations in pore structure. Their biocompatibility stems from the properties of the metal or substrate, rather than relying solely on their porous structure. PNMs have the advantage of being resistant to degradation by living organisms. Thus, they are widely applied in drug delivery, bioimaging, and biosensing, where the interplay between their

structure and function significantly influences the modulation of biological tissue and cellular functions. Herein, we review the reported research on the use of porous nanoparticles for various physiological mechanisms, such as drug delivery,<sup>7</sup> bioimaging,<sup>8,9</sup> and biosensing,<sup>4</sup> and their various applications in living organisms.

PNMs have the outstanding advantages of high loading capacity and tunable porosity, allowing different ligand modifications to create materials with specific targeting functions that can not only change shape or size but also have high sensitivity, high spatial resolution, and low toxicity for drug delivery and bioimaging. The inability of conventional oral drug delivery agents to deliver drugs at controlled release rates has generated interest and research in novel drug delivery methods. The developed drug delivery systems include polymer-based systems, MOF-based systems and mesoporous silicones. These different drug delivery routes are roughly classified into organic and inorganic systems. Organic systems such as polymer-based systems benefit from extensive biocompatibility and have the ability to absorb many drugs but lack controlled release mechanisms. Alternatively, inorganic delivery

<sup>a</sup> State Key Laboratory of Ultrasound in Medicine and Engineering, College of Biomedical Engineering, Chongqing Medical University, Chongqing 400016, P. R. China. E-mail: maox@cqmu.edu.cn

<sup>b</sup> Chongqing Key Laboratory of Biomedical Engineering, College of Biomedical Engineering, Chongqing Medical University, Chongqing 400016, P. R. China



materials such as MOFs can deliver adsorbed drugs at a controlled rate due to their ordered porous network but have a reduced loading capacity. Most inorganic delivery materials have a mesoporous structure for optimal drug uptake and delivery (microporous materials usually lack a pore size large enough for useful drug delivery).<sup>10</sup> As drug delivery systems, PNMs can deliver drugs, antigens and stimulatory molecules to target cells/tissues for cancer therapy through multiple pathways that modulate immune dysfunction in the tumor microenvironment.<sup>11,12</sup> Cancer immunotherapy using PNMs can avoid multi-drug resistance, reduce genetic mutations in tumor cells, and enhance synergistic therapeutic effects with other treatments such as chemotherapy, radiotherapy, photodynamic therapy (PDT), and photothermal therapy (PTT).<sup>13</sup> Furthermore, PNMs can be combined with other treatments such as PDT and PTT or used as radiosensitizers<sup>14</sup> to achieve better anti-cancer effects.<sup>15</sup> PNMs have inherent advantages such as high biomolecule loading capacity, adjustable structure, abundant surface modification and controlled release behavior of loading molecules such as immunomodulators.<sup>13,16,17</sup> They can enhance cancer immunotherapy by delivering antigen and stimulatory molecules to target cells/tissues, modulating immune dysfunction in the tumor microenvironment and promoting ACT therapeutic effects in various ways.<sup>11,18</sup>

The development of biomedical imaging technologies has greatly facilitated the diagnosis of various diseases. PNMs as imaging agents can generate signals or enhance the signal contrast of the target tissue for better diagnosis. Nanoparticle imaging agents for cancer diagnosis preferentially accumulate in tumors through EPR effects for passive targeting or through tumor-specific receptor binding for active targeting<sup>19</sup> and imaged using techniques such as positron emission tomography (PET), computed tomography (CT), ultrasound (US), and photo-acoustic imaging (PAI). The combination of fluorophores with PNMs also enables optical sensing and imaging of physiologically significant species. Usually, fluorescence imaging is influenced by the intensity of tissue autofluorescence in *in vivo* bioimaging. Various tissue components for example, elastin and collagen, and intracellular molecules for example, amino acids such as flavin, tyrosine and phenylalanine are known to act as endogenous fluorophores *in vivo*. These biological chromophores strongly absorb visible light and limit the excitation and emission of light in the visible spectral range based on the penetration depth. Other biological components such as water and lipids also strongly absorb light in the visible to infrared region.<sup>20</sup> The long-lived PL emission lifetime of PSiNP (typically in the order of a few microseconds) allows gated luminescence imaging to completely eliminate short-lived tissue autofluorescence, and thus gated luminescence imaging<sup>21</sup> can be effectively used for bioimaging. Other PNMs can be loaded with substances such as lanthanides to enable nanospatial resolution thermography, time-resolved fluorescence immunoassay, *etc.* Magnetic substances such as iron oxide, magnesium oxide porous nanoclusters and paramagnetic/superparamagnetic metal ions as ligands can be used as contrast agents for magnetic resonance imaging (MRI),<sup>22</sup> which have good biocompatibility and targeting properties, and also allow real-time monitoring of the contrast

agents due to their magnetic properties, demonstrating good prospects in bioimaging. In conclusion, PNMs show potential to overcome current barriers to cancer immunotherapy and enhance anticancer efficacy, and also are highly attractive for bioimaging.

A sensor is a device that converts quantitative or qualitative chemical or biochemical information into an analytically useful signal as a result of a chemical interaction or process between the analyte and sensor device. The use of specific and sensitive sensors to detect and monitor changes (electrical, electrochemical, optical and thermal signals) in biological elements (enzymes, antibodies, tissues or living cells) when they come in contact with sensitive materials can help diagnose diseases and reveal underlying biological problems.<sup>19</sup> These changes can be in the form of electrical (conductance, resistance and capacitance), electrochemical (conductance, amperage, impedance and potential), optical (reflection, photoluminescence and fluorescence) and thermal (temperature change) signals. Biosensors have a wide range of applications, including glucose monitoring, pathogen detection, quantitative measurement of toxicity and bioactivity assessment of new compounds.<sup>23</sup> Porous nanomaterials often have porous structures to allow the entry of multiple active substances (such as enzymes, proteins and molecules), and thus they can be applied in many different types of biosensors, allowing the analysis of many different types of biomolecules (such as enzymes) and their binding to specific targets,<sup>24</sup> such as label-free sensing substrates based on silicon nanowires for the detection of bilirubin<sup>25</sup> and the use of label-free electrochemical adaptive sensor with bimetallic hollow MOF for effective detection of adenosine.<sup>26</sup>

Therefore, it is of great significance to study the latest progress in biosensing and *in vivo* applications of porous nanoparticles and introduce their latest technologies. This article reviews the latest advances in various PNMs in medical applications such as drug delivery, bioimaging and biosensing, emphasizing the biocompatibility, degradability and flexibility of porous nanomaterials, making them suitable for *in vivo* applications through self-assembly pathways. This property shows great potential in the biomedical field, providing researchers with new possibilities. In the future, the application of porous nanomaterials is expected to achieve greater breakthroughs through more precise regulation of the size and shape of porous structures, and modification of their functional groups. Herein, we also emphasize the interdisciplinary nature of porous nanomaterials research, encouraging collaboration and interdisciplinary research to accelerate their development and innovation of their applications. These studies show that PNMs have great potential as an alternative to current clinical applications. Each section includes an in-depth discussion and summary of representative examples to highlight the wide range of applications of PNMs in the biomedical field. By analyzing the latest research trends, we also provide researchers with deep insight into the future direction of PNMs in the biomedical field. This not only provides scientists with a comprehensive understanding of the current status of PNMs in biomedicine, but also provides strong guidelines for future research and innovation.



Overall, porous nanomaterials show broad prospects for *in vivo* / *in vitro* applications and biosensing, providing strong support for the development of the medical field.

## 2. Silicon-based assembly materials

Porous silicon (PS) is a nanostructured material that offers a wealth of advantages to the current materials community. As its name implies, porous silicon is similar to quantum sponge, containing a meshwork of nanocrystals and pores.<sup>27</sup> Also, because silicon is readily available and inexpensive, it is an attractive and useful material for diverse applications. Porous silicon nanoparticles (PSiNPs) have outstanding properties including biocompatibility coupled with flexible pore morphology, structural properties, biodegradability, and unique optical and luminescent properties, making them preferable for drug delivery, bioimmunochemistry, bioimaging and biosensing applications (Fig. 1a).<sup>28</sup> It was shown that PSiNPs do not cause inflammatory responses in animal models and show good biocompatibility, gradually degrading to non-toxic silicic acid in aqueous media.<sup>29</sup> PSiNPs as drug delivery systems (DDS) have the advantages of high loading, good biocompatibility, and ease of functionalization (Fig. 1b), where their unique properties and advantages as nanomedicines can be summarized as follows:

(1) they can be used as multifunctional platforms or therapeutic agents for diagnosis and treatment by integrating multiple imaging techniques; (2) their large specific surface area and internal volume allow for simple immersion or chemical adjuvant loading to introduce large amounts of cargo; (3) ligand modifications can be used as physicochemical optimization of targeted drugs and nanoparticles, allowing simultaneous drug delivery and imaging of targeted disease sites; and (4) fine-tuned control of PSiNPs to increase circulation time in the blood by reducing the conditioning effect and uptake of the mononuclear phagocytic system (MPS).<sup>30</sup> To date, poor water solubility remains a major factor limiting the efficacy of drugs; accordingly, by incorporating drug molecules in PSiNPs, premature drug degradation can be effectively prevented while maintaining complete control of the drug release.<sup>31</sup> PSi nanodrug delivery has abundant flexibility to achieve drug delivery by oral, intravenous or subcutaneous administration, and accordingly, it is predicted that lower doses of conventional anticancer agents can be used to achieve better therapeutic results.<sup>32</sup> Furthermore, PSiNPs can be used as subcutaneous implants to deliver trace minerals such as iodine, selenium, chromium, manganese and molybdenum as dietary supplements and other therapeutic agents such as lithium for depression, gold and silver with antimicrobial properties or platinum and palladium for oncologic diseases.<sup>33</sup>

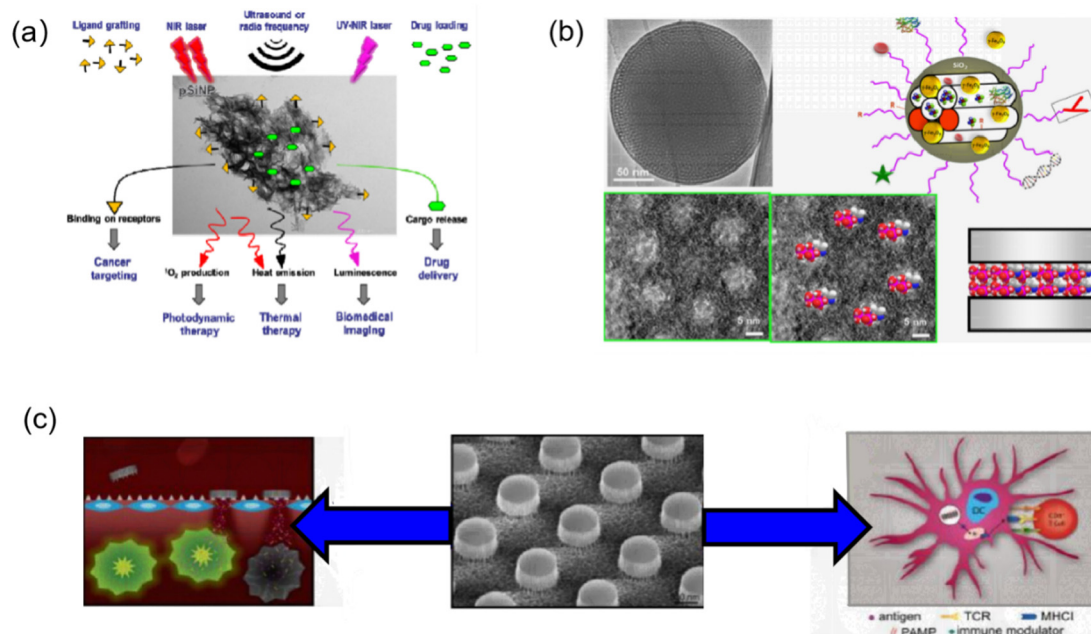


Fig. 1 (a) Multifunctionalities of PSiNPs for cancer theranostics. (b) Schematic illustration of drug loading in the mesopores of mesoporous silica nanoparticles (MSNs). Top left image: Transmission electron micrograph of MSN. Top right illustration: Schematic depiction of an MSN showing its role as a versatile multifunctional nanoplatform. Bottom left image: Enlargement of the above-mentioned image, where the ordered hexagonal arrangement of the pores to be loaded is clearly seen. Bottom center: Depiction of drug molecules loaded in mesoporous channels. Bottom right: Schematic representation of a horizontal perspective of silica channel loaded with drug molecules. (c) Schematic overview presenting porous silicon microparticle fabrication and applications in drug delivery and immunotherapy the central image is a scanning electron micrograph showing a patterned pSi wafer prior to sonication-based release of the patterned particles. The multistage vector concept of drug delivery is shown on the left, with intravascular administration of pSi particles resulting in tumor-associated vascular accumulation based on geometric properties, charge or targeting ligands. Images reprinted with permission from Bimbo *et al.* (2010, ACS), Kulyavtsev *et al.* (2017, *Pharm. Pat. Anal.*) and Serda *et al.* (2015, US8926994), respectively.



The Jeong research group utilized the condensation chemistry of calcium silicate to load the rheumatoid arthritis drug methotrexate (MTX) in PSiNPs. Systemic administration of the constructs formed by PSiNPs loaded with MTX, known as pCaSiNPs, resulted in its accumulation in inflamed joints, leading to improvements in the progression of rheumatoid arthritis in both early and established stages. The biological degradation products of the pCaSiNP drug carrier exhibit immunomodulatory and anti-absorptive effects, emphasizing their crucial role in the biocompatibility of implantable devices.<sup>34</sup> Studies on the different pathways of absorption, distribution and excretion in mice have shown that PSiNPs have good tissue biocompatibility for oral and intravenous administration.<sup>35</sup> PSiNPs have been shown to deliver large biomolecules that can be used for immunotherapy (Fig. 1c). Zhang *et al.* from Wuhan University co-loaded silica nanoparticles with a hypoxia-activated prodrug (HAP) and a vascular disruptor, and then coated the particles with platelet membranes. Once in the tumor, this nanotherapy could disrupt local blood vessels, and thus inhibit the tumor.<sup>36</sup> Ferrari *et al.* of the Methodist Hospital Research Institute developed PSiNPs functionalized with toll-like receptor ligands as adjuvants for anticancer immunity. It was shown that mesoporous PSiNPs conjugated with lipopolysaccharide (LPS) or monophospholipids could be readily internalized by dendritic cells.<sup>37</sup>

The Sailor group used the optical properties of PSiNPs to design immune protocols by loading antigens in luminescent PSiNPs (LPSiNPs). The antigens were loaded in PSiNPs with antibodies that are designed to selectively target and induce T cell-mediated immune responses.<sup>38</sup> Kim *et al.* proposed that nanoparticles can target activated macrophages and loaded them with siRNAs targeting the Irf5 gene. This formulation could induce >80% gene silencing in activated macrophages *in vivo* and inhibit excessive inflammatory responses, producing significantly improved therapeutic outcomes in a mouse model of bacterial infection.<sup>39</sup>

The unique advantages of PSiNPs, such as good compatibility, inherent photoluminescence (PL), high surface area and ease of surface functionalization, make PSiNPs-based contrast agents (CAs) clinically suitable for biomedical imaging.<sup>40</sup> The high surface area of PSiNPs allows the loading of different CAs for different imaging modalities. The potential bioimaging methods using PSiNPs include optical imaging, MRI, positron emission tomography (PET), and single-photon emission computed tomography (SPECT) imaging. Cunin *et al.* successfully constructed multifunctional PSiNPs to deliver Ru(II) complex photosensitizers for near-infrared imaging and photodynamic therapy (PDT).<sup>41</sup> Powerful NIR imaging capabilities and effective inhibition of cell growth were observed *in vitro* under NIR irradiation. Zabotnov *et al.* used picosecond laser ablation of

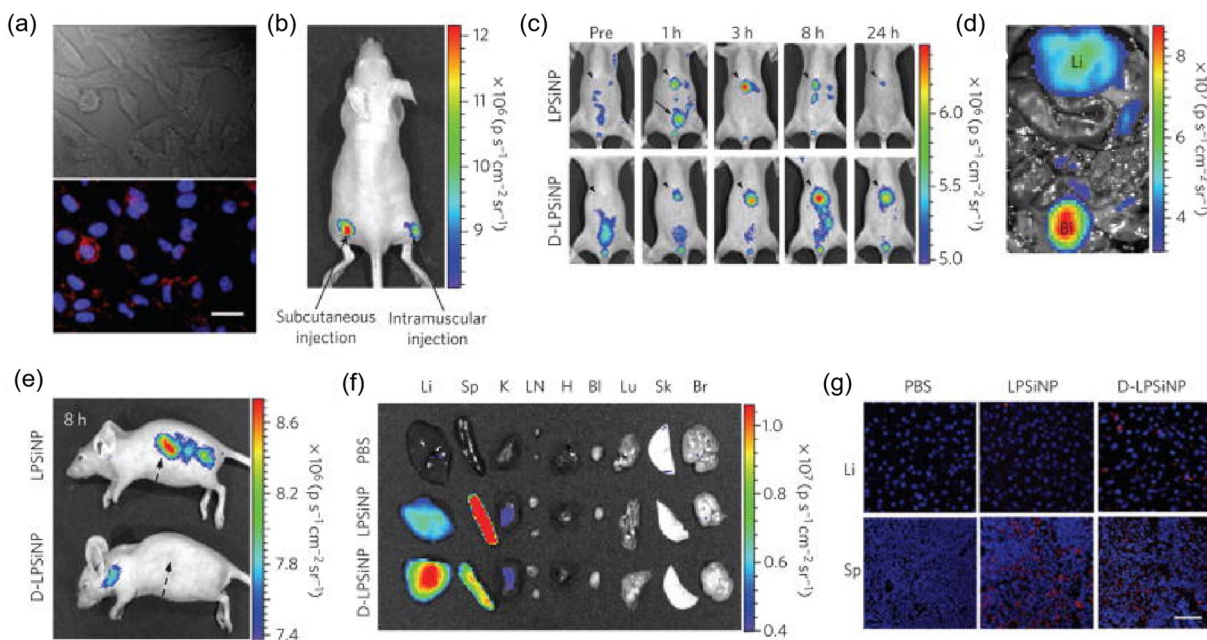


**Fig. 2** (a) *In vitro* cellular imaging with LPSiNPs. HeLa cells were treated with LPSiNPs for 2 h, and then imaged. Red and blue indicate LPSiNPs and cell nuclei, respectively. The scale bar is 20  $\mu$ m. (b) *In vivo* fluorescence image of LPSiNPs ( $20 \mu$ L of  $0.1 \text{ mg mL}^{-1}$ ) injected subcutaneously and intramuscularly on each flank of a mouse. (c) *In vivo* images of LPSiNPs and D-LPSiNPs. The mice were imaged at multiple time points after intravenous injection of LPSiNPs and D-LPSiNPs ( $20 \text{ mg kg}^{-1}$ ). Arrowheads and arrows with solid lines indicate liver and bladder, respectively. (d) *In vivo* image showing the clearance of a portion of the injected dose of LPSiNPs in the bladder, 1 h post-injection. Li and Bl indicate liver and bladder, respectively. (e) Lateral image of the same mice shown in (c), 8 h after LPSiNP or D-LPSiNP injection. Arrows with dashed lines indicate spleen. (f) Fluorescence images showing the ex vivo biodistribution of LPSiNPs and D-LPSiNPs in a mouse. Organs were collected from the animals shown in (c), 24 h after injection. Li, Sp, K, LN, H, Bl, Lu, Sk and Br indicate liver, spleen, kidney, lymph nodes, heart, bladder, lung, skin and brain, respectively. (g) Fluorescence histology images of liver and spleen from the mice shown in (c) and (f), 24 h after injection. Red and blue indicate (D-)LPSiNPs and cell nuclei, respectively. The scale bar is 50  $\mu$ m for all images. Images reprinted with permission from Park *et al.* (2009, *Nat. Mater.*).



porous silicon films and nanowires to synthesize small silicon nanoparticles (14–65 nm) with fluorescence emission in the NIR range (600–1000 nm), which created a new prospect for use as optical imaging contrast agents.<sup>42</sup> Xia *et al.* fabricated PSiNPs@Fe<sub>3</sub>O<sub>4</sub> nanocomposites for dual-mode imaging by covalently bonding superparamagnetic Fe<sub>3</sub>O<sub>4</sub> NPs with photoluminescent PSiNPs.<sup>43</sup> In this nanocomposite, PSiNPs were used as the NIR imaging agents and Fe<sub>3</sub>O<sub>4</sub> NPs the CAs for MRI. This nanocomposite exhibited good biocompatibility and performed well in fluorescence/MR bimodal imaging of cells *in vitro* and tumors *in vivo*. Microsecond photoluminescence is a unique feature of PSiNPs for bioimaging. Kim *et al.* reported the fabrication of iRGD-PEG-modified PSiNPs for two-photon imaging of living animals. By limiting the size of PSiNPs to 60 nm and increasing the two-photon absorption cross section, the photoluminescence intensity of NPs and the signal-to-noise ratio of two-photon imaging significantly improved.<sup>2</sup> In addition, the tumor-targeting effect of 60 nm PSiNPs-iRGD was confirmed by experiments in a mouse orthotopic HeLa tumor model. Park *et al.* used dextran-coated LPSiNPs (D-LPSiNPs) for tumor imaging, demonstrating luminescent porous silica nanoparticles (LPSiNPs) that can carry drug payloads with inherent near-infrared photoluminescence capable of monitoring accumulation and degradation *in vivo* (Fig. 2) with low toxicity degradation pathways suitable for *in vivo* applications.<sup>44</sup> Overall, PSiNP-based nanosystems have great potential for bioimaging, given that their long-lived photoluminescence can be utilized to eliminate the interference of tissue autofluorescence. This

enhances the differentiation of CA from endogenous fluorophores of living tissues.

PSiNPs have captivating and tunable features including easy fabrication, special optico-physico properties, tailored morphological structure and versatile surface chemistry enhancing their prospects as a transducer for the fabrication of biosensors. Furthermore, PSiNPs can be used for other biomedically relevant assays such as glucose, DNA, bacteria, viruses and proteins. Syshchyk *et al.* fabricated biosensors for the determination of glucose and urea based on the fact that the photoluminescence of porous silicon varies with the pH of the medium.<sup>45</sup> Experiments showed that the photoluminescence intensity of porous silicon increased by 1.7-fold when the glucose concentration increased from 0 to 3.0 mM, whereas it decreased by 1.45-fold when the urea concentration was increased to the same level. Also, the presence of heavy metal ions (Cu<sup>2+</sup>, Pb<sup>2+</sup> and Cd<sup>2+</sup>) in the solution inhibited the enzymatic reactions catalyzed by glucose oxidase and urease, thus restoring the photoluminescence quantum yield of porous silicon, and thus this biosensor could also be applied for the inhibition analysis of heavy metal ions (Fig. 3a). Zhang *et al.* proposed a non-spectral porous silicon optical biosensor technique based on dual-signal light detection of the concentration of DNA molecules.<sup>46</sup> In the dual-signal light detection method, the first detection signal light is the detection light reflected from the surface of a porous silicon Bragg mirror. The second detection signal light is fluorescence, and the Bragg mirror structure further enhances the fluorescence signal. After receiving digital images of the two signal

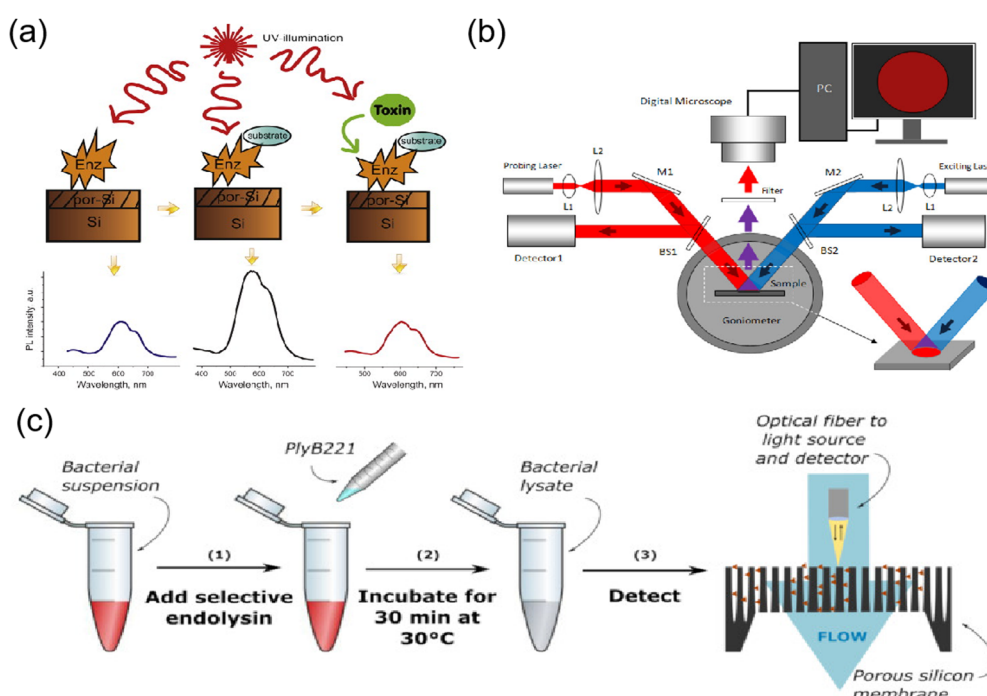


Fig. 3 (a) Schematic of luminescent biosensors based on GOD or urease for the detection of glucose, urea and heavy metals. (b) PSi optical biosensor with different concentrations of DNA by the double-signal optical detection mechanism. (c) Protocol for the detection of bacteria on a PSi membrane. Images reprinted with permission from Syshchyk *et al.* (2015, *Biosens. Bioelectron.*), Zhang *et al.* (2022, *Sensors (Basel, Switzerland)*) and Vercauteren *et al.* (2021, *Biosensors*), respectively.



lights superimposed on the porous silicon surface simultaneously using a digital microscope, a corresponding algorithm is used to calculate the change in the average gray value before and after the hybridization reaction to calculate the concentration of DNA molecules (Fig. 3b). This method allows the detection of target DNA not only by hybridization, but also by immunoreactivity or parallel biochips with porous silicon biosensors to detect antigens. Vercauteren *et al.* used PSi membranes (PSiMs) for the optical detection of *Bacillus cereus* lysates (Fig. 3c). Prior to detection, the bacteria were selectively lysed by PlyB221, an endolysin encoded by Deep-Blue, which is a phage targeting *Bacillus cereus*. This detection platform not only enabled the rapid detection of bacteria, but the same technique could be extended to other bacteria by selective lysis, such as the detection of *Staphylococcus epidermidis* and selective lysozyme lysis.<sup>47</sup> Layouni *et al.* combined peptides with a multifunctional PSi optical biosensor platform for the detection of the chikungunya virus E2 protein. Peptide functionalization and selective E2 protein capture were confirmed by contact angle measurements, attenuated total reflection-Fourier transform infrared spectroscopy and optical reflectance measurements, and this biosensor could be exposed to high-temperature environments.<sup>48</sup>

### 3. Porous assembly structures based on metal organic frameworks (MOFs)

Since the pioneering work by Yaghi's in 1995,<sup>49</sup> an increasing number of researchers have been focused on the design and

application of MOFs. Metal-organic frameworks (MOFs) are constructed based on organic and inorganic building blocks, with vacant spaces (pores) arising between individual structural units. As a new class of porous organic-inorganic crystalline hybrid materials, MOFs are dominated by the self-assembly of metal atoms and organic backbones, and some functional species including small biomolecules, metal ions, and magnetic groups can be loaded in the pores of the framework to confer functions. In addition, some MOFs containing lanthanides or luminescent organic ligands can generate fluorescence or phosphorescence under UV light.<sup>1</sup> Due to these superior properties of MOFs, they have been widely used in different types of applications such as sensing,<sup>50</sup> drug delivery,<sup>51</sup> bioimaging<sup>52–54</sup> and other bio-related applications.<sup>55</sup>

Metal organic backbones (MOFs) with luminescent properties and size- or shape-selective adsorption properties can be used as sensor devices. nMOF-based sensors can satisfy the requirements of high sensitivity, resolution and accuracy for cellular biosensing. The pH dysregulation of intracellular fluids is associated with tumorigenesis and drug resistance, and real-time sensing and monitoring of intracellular pH changes in living cells is important for exploring disease mechanisms and designing pH-responsive intracellular drug delivery systems. Lin and colleagues reported the first nMOFs for real-time intracellular pH sensing.<sup>56</sup> A fluorescein moiety was attached to Zr-based UiO nMOFs *via* thiourea bonds, with two excitation wavelengths (435 *vs.* 488 nm) associated with pH-dependent relative fluorescence intensity. They were imaged by live cell confocal microscopy to illustrate the acidification process

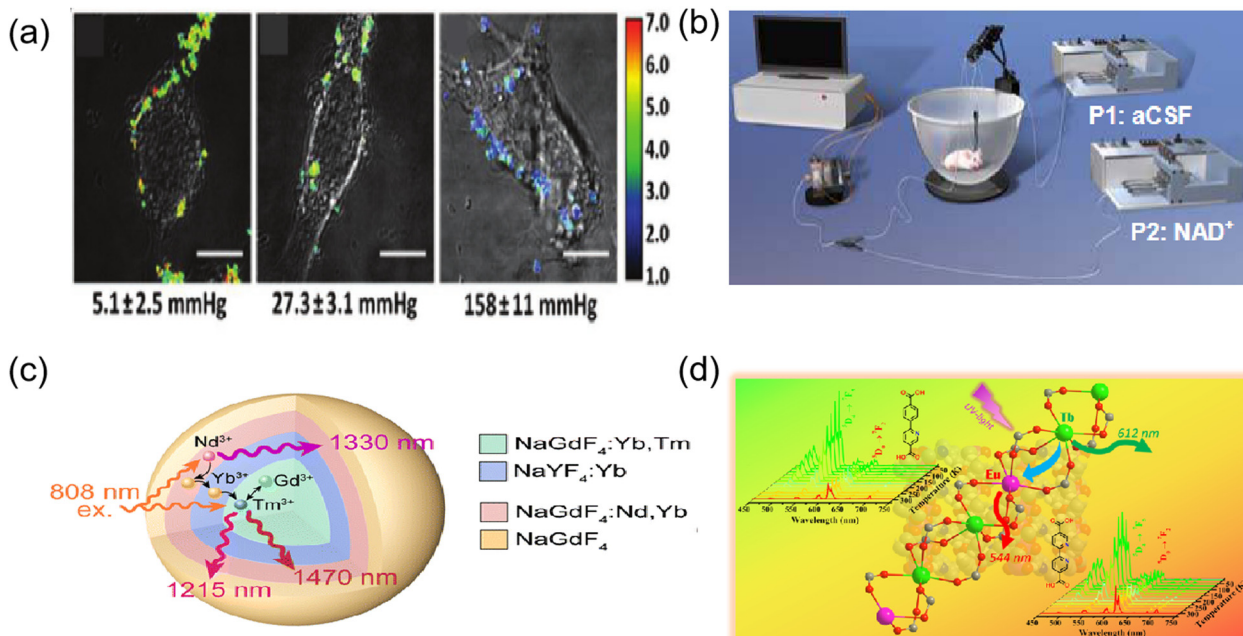


Fig. 4 (a) Ratiometric imaging of CT26 cells incubated with biosensor based on R-UiO under hypoxia (left), normoxia (middle), and aerated (right) conditions. (b) Schematic illustration of the online electrochemical detecting system for *in vivo* monitoring of glucose in cerebral system. (c) Schematic of the NaGdF<sub>4</sub>:Yb, Tm@NaYF<sub>4</sub>:Yb@NaGdF<sub>4</sub>:Yb, Nd@NaGdF<sub>4</sub> nanocomposite as a dual ratiometric luminescence nanothermometer (DRLNT). (d) Characterization of Ln<sup>3+</sup>-based metal-organic frameworks (LnMOFs) compounds by single-crystal X-ray diffraction (XRD), powder XRD, and thermogravimetric analysis. Images reprinted with permission from Xu *et al.* (2016, *J. Am. Chem. Soc.*), Ma *et al.* (2013, *Anal. Chem.*), Hu *et al.* (2022, *Nanoscale Horiz.*) and Zhao *et al.* (2019, *Inorg. Chem.*), respectively.



during endosome maturation with high spatial resolution and fast temporal response. Various diseases, such as cancer and vascular diseases, can lead to tissue hypoxia and reduced oxygen levels. Therefore, intracellular oxygen sensing is important for the diagnosis and treatment of cancer. Lin *et al.* designed the first phosphorescent/fluorescent dual-emission nMOF for intracellular oxygen quantification.<sup>57</sup> A hybrid ligand M-nMOF containing the oxygen-responsive phosphorescent ligand Pt-5,15-bis(*p*-benzoate) porphyrin and the amino-functionalized ligand amino-quaternary ammonium phenyl dicarboxylic acid was first synthesized. Subsequently, rhodamine B was covalently attached to the amino group *via* a thiourea bond as an oxygen-independent reference to provide R-nMOF. These two chromophores share the same excitation energy, while their phosphorescent/fluorescent emission does not interfere with each other. Subsequently, a ratiometric photoluminescence method for quantifying oxygen was established, allowing the confocal microscopic imaging of living cells by R-nMOF to determine the oxygen levels in hypoxic, normoxic, and aerated cells (Fig. 4a). Several metal ions play a key role in cellular activity, but their presence at high concentrations can be toxic and lethal. Accordingly, the selective detection of metal ions in cells is required for diagnostic purposes. Because energy/charge transfer between ligands and metal ions leads to fluorescence burst, MOFs can carry the corresponding ligands for their detection. Lu *et al.* developed nMOF-253 with 2,2'-bipyridine-5,5'-dicarboxylic acid (bpydc) ligands for the detection of  $\text{Fe}^{2+}$ .<sup>58</sup> The fluorescence of the ligand was selectively burst by  $\text{Fe}^{2+}$ , which is probably due to light-induced electron transfer, allowing nMOF to be used for intracellular  $\text{Fe}^{2+}$  sensing in HeLa cells. NMOF-based systems have also been developed for the detection of the metal ion  $\text{Cu}^{2+}$  based on the luminescence burst of  $\text{Tb}^{3+}$  ions.<sup>59</sup>

Ma *et al.* prepared an integrated dehydrogenase electrochemical biosensor (Fig. 4b) based on zeolitic imidazolate frameworks (ZIFs) as a substrate for the construction of an integrated dehydrogenase electrochemical biosensor with high sensitivity to glucose for *in vivo* measurement of neurochemicals.<sup>60</sup> It was demonstrated that ZIFs are capable of acting as substrates for immobilizing electrocatalysts (*i.e.*, methylene green, MG) and dehydrogenases (*i.e.*, glucose dehydrogenase, GDH) on the electrode surface, exhibit excellent adsorption capacity for MG and GDH, and are easy to form integrated electrochemical biosensors, and thus were used as substrates for our glucose biosensor. The ZIF-based biosensor was shown to be more selective for glucose than other endogenous electroactive substances in the brain system and could selectively monitor dialysate glucose collected from guinea pig brains in a near real-time mode.

In the case of Ln-based nMOFs, as thermal probes, they were evaluated as multifunctional luminescent thermometers, which are luminescent mixed lanthanide MOF thermometers capable of directly visualizing temperature changes with an excellent linear correlation between temperature and luminescence intensity ratios in the range of 50–200 K.<sup>61</sup> This was first investigated on the microscale, and more recently on the

nanoscale. Zhao *et al.* prepared two types of isostructural  $\text{Ln}^{3+}$ -based metal-organic skeletons under solvent heating conditions, in which two structurally similar pyridine-containing dicarboxylic acid ligands, *i.e.*, 6-(4-carboxyphenyl)nicotinic acid and [2,2'-bipyridyl]-5,5'-propanedioic acid, were used as organic connectors. Two hybrid LnMOFs, namely,  $\text{Tb}_{0.95}\text{Eu}_{0.05}$  cpna and  $\text{Tb}_{0.95}\text{Eu}_{0.05}$  bpydc, were obtained by the lanthanide co-doping method and evaluated for their application as proportional luminescence thermometers.<sup>62</sup> It was experimentally confirmed that both materials exhibited a good S-shaped response in the temperature range of 25–300 K with good relative sensitivity and temperature uncertainty (Fig. 4d). In addition, their color changes from green at 25 K to red at 300 K make them suitable as colorimetric luminescence probes. Hu *et al.* used a rare earth-doped nanocomposite of  $\text{Tm}^{3+}$  and  $\text{Nd}^{3+}$  ions as emitters to construct a dual-scale LNT.<sup>63</sup> A strategy for enhanced  $\text{Tm}^{3+}$  NIR radiation for bioimaging-based *in vivo* temperature detection was developed using cross-relaxation processes between lanthanide ions (Fig. 4c). The dual-ratio probe components in the nanocomposites have the potential to monitor temperature differences and heat transfer at the nanoscale, which will help regulate heating operations more precisely in thermotherapy and other biomedical applications. This work not only provides a powerful tool for *in vivo* temperature sensing, but also presents a method for building highly efficient NIR-II/III rare earth luminescent nanomaterials for a broader range of biological applications. These pioneering studies highlight the possibility of using nano MOFs for monitoring physiological temperature in medical applications, which can be further explored with nanoscale hybrid rare earth MOFs. These novel luminescent thermometers can be further applied in the near future as nanothermometers for intracellular sensing and thermal imaging with nanospatial resolution.

Inspired by early studies on the development of polymer-based drug delivery systems, several researchers have attempted to develop MOF-based nanoparticles as drug carriers for targeted cancer therapy.<sup>64–66</sup> MOFs have unique advantages as potential drug carriers, as follows: (1) highly tunable properties and porosity, (2) high drug loading capacity, and (3) controlled multifunctionality. MOF-based drug delivery systems such as pH-responsive delivery systems, magnetically guided delivery systems, folate-targeting delivery systems, and temperature-responsive delivery systems have been developed. Various structures of MOFs are available as carriers for different drugs, some of which have a loading capacity of up to  $81.6\% \pm 0.6\%$ .<sup>67</sup> Choudhuri *et al.*<sup>68</sup> designed a pH-responsive DDS drug delivery system that can be used to construct multifunctional nanoparticles in a simple and rapid way, which combines upconversion nanoparticles (UCNPs) and MOFs. The outstanding advantages of encapsulated targeting (Fig. 5a) make it suitable for releasing drug molecules in the tumor region. We adsorbed 5-FU as a model drug in UCNPs@ZIF-8/FA nanocomposites at 37 °C and pH 5.5 and 7.4. Finally, we observed that the 5-FU release process has a significant pH response, as shown in Fig. 5b. This showed that the release behavior of 5-FU changed significantly under different pH environments, highlighting the controllability of the nanocomposite in drug release. Ke *et al.* reported the synthesis of a core–shell



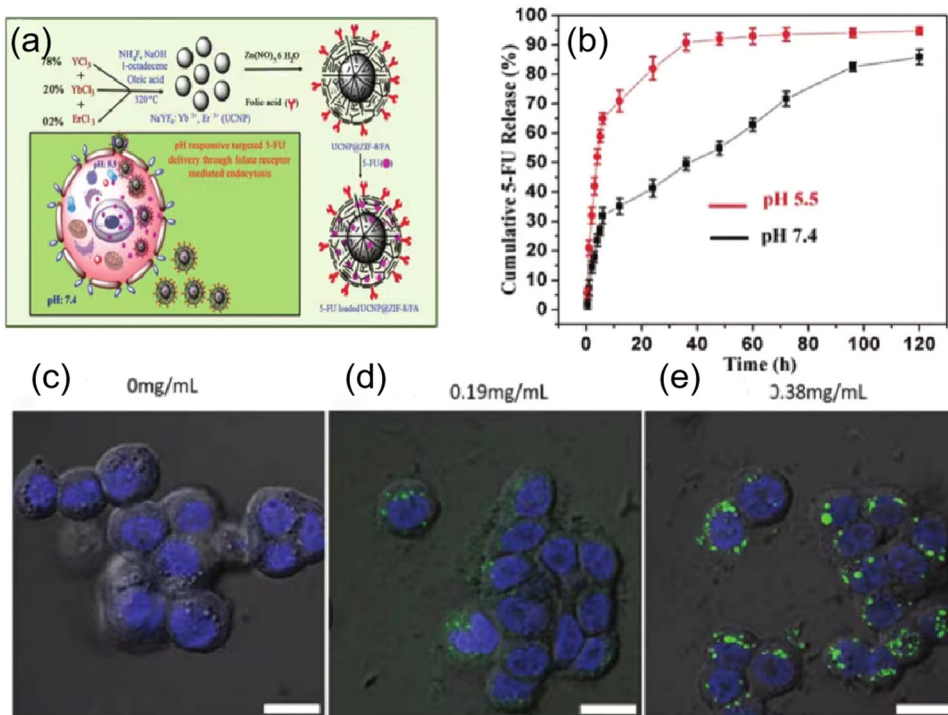


Fig. 5 (a) Schematic representation of encapsulated process of upconversion NMOFs modified with folic acid and pH responsive drug delivery (left). (b) *In vitro* 5-FU release profiles from 5-FU@UCNP@ZIF-8/FA measured at pH 5.5 and 7.4 at  $37^\circ\text{C}$  (right). (c) and (d) Confocal fluorescence images of the DRAQ5 channel (blue, nuclear stain) and the BDC-NH-BODIPY channel (green) of HT-29 cells incubated with no particles 0.19 mg mL<sup>-1</sup> and 0.38 mg mL<sup>-1</sup> particles, respectively. (e) Confocal microscopy images of H460 cells incubated with various nanoparticles. Images reprinted with permission from Xiao *et al.* (2011, *J. Mater. Chem.*), Taylor-Pashow *et al.* (2020, *JCIM*) and Xu *et al.* (2009, *J. Am. Chem. Soc.*), respectively.

nanomaterial ( $\text{Fe}_3\text{O}_4@\text{MOF-5}$ ) consisting of  $\text{Fe}_3\text{O}_4$  nanorods (magnetite) and nanocrystals of MOF-5.<sup>69</sup> Nimesulide was selected as the model drug and loaded in the pores of  $\text{Fe}_3\text{O}_4@\text{MOF-5}$ . The experimental results showed that a high drug loading rate was achieved (20 wt%), while the incorporated drug exhibited a rapid response to a magnetic field. Magnetic drug delivery (MDD) is one of the most promising targeting drug delivery systems. With the help of external magnetic conditions, magnetic drug agents can be precisely targeted to a specific location, while magnetic properties also allow the real-time monitoring of magnetic agents, which can be used as contrast agents for bioimaging.<sup>70</sup> The folate receptor (FR) is overexpressed in some tumor tissues, and when MOFs are encapsulated by folic acid, they will be carried into the cell and take up folic acid more readily than in normal tissues. For example, Li *et al.* reported the synthesis of a nanoscale metal-organic framework, DOX@UiO-68-FA, which was decorated with UiO-68 and folic acid.<sup>70</sup> They performed cell biocompatibility and membrane permeability experiments to demonstrate that DOX@UiO-68-FA had higher cellular uptake in Hep G2 cells compared to DOX@Mi-UiO-68 and free DOX. Furthermore, the *in vivo* antitumor assays showed that among free DOX, DOX@Mi-UiO-68 and DOX@UiO-68-FA, DOX@UiO-68-FA exhibited the highest antitumor effect in PBS. Tavakolizadeh *et al.* designed a novel UiO-66 MOF and MXene nanocomposite modified with rosemary (RO) leaf extract to co-deliver doxorubicin (DOX)/clustered regularly spaced short palindromic repeats (CRISPR). For the first time, the synthesis

of nanomaterials was completed with the aid of a super-gravity system and a rotating packed bed device. The modeling results confirmed the successful synthesis of the nanomaterials. Based on the drug release and loading results, the DOX payload efficiency of around 46% was recorded and sustained drug release at acidic pH (the same as cancer cells) was observed.<sup>71</sup> Wang and colleagues constructed a nanoscale metal-organic framework, CaZol, using zoledronic acid and calcium, and then targeted by drug-free Fol liposomes to incorporate folic acid as a targeting ligand in CaZol.<sup>72</sup> The cellular uptake experiments showed that Fol-targeting CaZol showed a higher uptake efficiency than non-targeting CaZol in H460 and PC3 cells. Also, the biodistribution experiments in thymus-free nude mice showed that Fol-targeting CaZol accumulated in tumors at higher amounts than non-targeting CaZol under the same conditions. The temperature *in vivo* usually does not vary significantly, and in this case, temperature-responsive drug carriers can be manufactured based on an external thermal field. For example, Lin *et al.* synthesized two MOFs, ZJU-64 and ZJU64-CH<sub>3</sub>, using zinc nitrate, adenine and carboxylate ligands. Methotrexate (MTX) was added to these MOFs as a model drug according to the impregnation method.<sup>73</sup> In the drug release assay, methotrexate was released from the framework and exhibited temperature-responsive phenomena. When the release progress was measured at  $60^\circ\text{C}$ , ZJU-64 and ZJU64-CH<sub>3</sub> released MTX from their frameworks in approximately 1.5 and 6 h, respectively, which is equal to the amount released at  $37^\circ\text{C}$  for 72 h. At present, only a few studies have been reported on the

thermo-responsive release of MOF-based drug carriers, which may be due to the fact that the *in vivo* temperature is basically stable at 37 °C and it is difficult to realize significant changes to trigger drug release.

MOFs have attracted great interest in the field of bioimaging due to their easy intracellularization, good dispersion stability and good bioavailability. Also, the surface of MOFs can be decorated with silica, organic polymers and lipid bilayers to improve their stability and confer biocompatibility.<sup>74</sup> Thus, new hybrid materials can be used as contrast agents for magnetic resonance imaging (MRI) by incorporating a large number of paramagnetic/superparamagnetic metal ions. For example, Wilasinee and colleagues reported the synthesis of a Gd-based NMOF as a contrast agent for MRI.<sup>75</sup> A simple route to control nanoparticles such as sodium salicylate (NaSal), salicylic acid and their derivatives, and other hydrophobic compounds were used in the synthesis process, as shown in this paper. Most NMR studies demonstrated that Gd-based MOF nanoparticles show higher *T* relaxation than conventional magnetic materials. Some MOFs with luminescent building blocks (ligands or metal ions) or bound fluorescein can be used for optical imaging (OI). Lin *et al.* reported the preparation of an Fe(III)-based MOF with 2-aminoterephthalic acid, whose structure is very similar to MIL-101.<sup>76</sup> An optical contrast agent (BODIPY dye) and an ethoxysuccinic acid-cisplatin anticancer prodrug were successfully integrated in the NMOFs by post-synthetic modification. To evaluate the *in vitro* effect of this nanoparticle as an optical contrast agent, a laser scanning confocal microscopy study was performed on HT-29 human colon adenocarcinoma cells. The results showed that the fluorescence of BODIPY appeared in the cells incubated with the nanoparticles, while no fluorescence was observed in the control group (Fig. 5c–e). These results suggest that nano-sized MIL-101 (iron) particles provide an effective platform for delivering optical contrast agents *in vitro*. MOF optical imaging probes are limited by their poor penetration and difficulty reaching the interior of cells. However, the rational combination of an imaging modality and contrast agent can provide advantages in intraoperative imaging and image-guided cancer surgery. Iodinated ligands or iodide loads can be used for X-ray computed tomography. Zhang *et al.* found that MOF nanocrystals containing iodine-boron diphenyl ether (BODIPY), which are known as UiO-PDT, exhibited strong X-ray attenuation in *in vitro* CT imaging and preferentially aggregated at tumor sites. More importantly, no significant side effects were observed for this nanocrystal at all the tested injection doses.<sup>77</sup>

## 4. Porous polymer membranes

Porous polymer membranes show great potential for biological and biomedical applications such as tissue engineering, bioseparation and biosensing due to their structural flexibility, multiple surface chemistry and biocompatibility.<sup>78</sup> Furthermore, due to their unique properties, such as tunable pore size and shape, density, and large surface-to-volume ratio, they can bind a large

number of functional groups in their pores and have a wide range of applications, including separation, such as water filtration and hemodialysis, support scaffolds, such as tissue engineering, and diagnostic tools, such as sensing platforms.<sup>79,80</sup> Fig. 6a presents a summary of the latest technologies and future prospects for the biomedical applications of polymeric membranes. The biocompatibility and biodegradability of membranes are crucial factors for their application.<sup>81</sup> Surface properties determine the degree of biocompatibility, and thus the membrane surface must often be modified to enhance its interactions with biological samples or inhibit immune responses.<sup>82</sup>

One of these drug delivery systems (DDS) has been extensively studied, given that controlled drug delivery to the target site is currently in great demand to reduce the serious side effects that occur when drugs come into direct contact with normal cells. The current drug delivery methods are mainly intravenous and oral. However, these methods have important drawbacks such as poor drug solubility and biodistribution, rapid drug breakdown, and extravasation of tissue damage. DDS aims to reduce these drawbacks by maximizing the therapeutic efficacy, drug release time, and drug stability in the body, increasing the bioavailability and reducing the adverse effects of drugs.<sup>83</sup> Porous polymer membranes are used in DDS to control the diffusion of drug molecules by regulating their permeation and drug release. Yang *et al.* prepared cylindrical nanochannels *via* the self-assembly of PS-*b*-PMMA block copolymers to demonstrate the biotherapeutic, controlled release of human growth hormone (hGH) *in vitro* and *in vivo*.<sup>84</sup> As shown in Fig. 6b, the porous polymer membranes induced fibroblast chemotaxis and hemostasis for wound healing with a lower immune response compared to many other synthetic polymers (e.g., polystyrene and polyethylene).<sup>85–88</sup> For use in tissue engineering, biopolymer membranes have several advantages compared to synthetic membranes in that they offer good biocompatibility, biodegradability, inherent bioactivity, ability to attract cells, and susceptibility to cell-triggered protein degradation and natural remodeling.

Polymers are ideal materials for the fabrication of disposable biosensors and are beneficial for biomedical applications. Porous polymer membranes can be used in biosensor strategies to limit the diffusion of interfering high-molecular-weight biological agents (e.g., large proteins), while still allowing the diffusion of low-molecular-weight solutes (e.g., metabolites) to the surface of the sensor for their detection.<sup>89</sup> They can also selectively capture target analytes by interacting with bioreceptors immobilized on the surface of the nanopore/nanochannel.<sup>90,91</sup> Porous polymer membranes can be used to modify the surface of working electrodes to improve their sensitivity, for example, by introducing nanoscale pores that not only increase the surface area but also can be used as nanopores where biometric events can be confined, maximizing binding compared to the use of conventional non-nanostructured electrodes. These pores can also be used as filters to minimize interference.<sup>92,93</sup> Fig. 6c and d depict an example of a sensing platform that utilizes nanopore plugging caused upon analyte binding as the sensing mechanism, as well as the expected



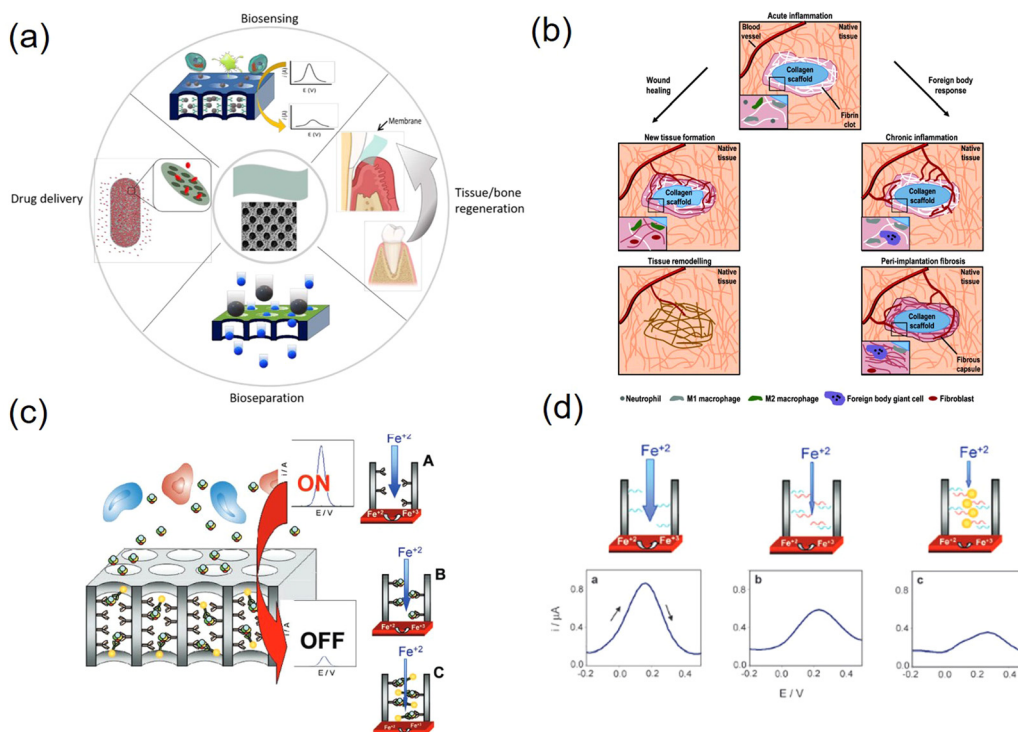


**Fig. 6** (a) Overview of biomedical/biological applications of porous polymeric membranes. (b) Mechanism of the two possible pathways of acute inflammation. In acute inflammation neutrophils, monocytes, and macrophages are observed. The left scheme corresponds to a wound healing process and the right scheme corresponds to a foreign body response. In wound healing, tissue remodelling occurs at the end of the process. In foreign body response, acute inflammation remains for a long period. (c) Mechanism of nanochannel blockage electrochemical sensing. (d) Differential pulse voltammograms (DPVs) of (a) only bioreceptor is attached on the channel walls and (b) after target analytes are captured by the bioreceptor and block the pores. Images reprinted with permission from Shiohara *et al.* (2020, *J. Mater. Chem. B*), Delgado *et al.* (2015, *Tissue Eng., Part B*), de *et al.* (2011, *Small*) and de *et al.* (2010, *Chem. Commun.*), respectively.

electrochemical response. Bioreceptors are immobilized on nanopore structures ready to bind to the target analyte, resulting in changes in the measured electrochemical signal due to partial nanopore blockage.<sup>94,95</sup> Sadeghi *et al.* reported a unique method for the electrostatic separation of organic molecules of similar size based on their creation of nanoporous membranes with filled arrays of polymer micelles in alcohol.<sup>96</sup> Overall, the combination of porous polymer membranes with other technologies to dope other materials or explore new polymeric materials with special properties such as high conductivity and high electrocatalytic activity adds new opportunities and may also help overcome the drawbacks of each technology and the disadvantages of porous polymer membranes such as poor stability at high temperatures or in organic solvents, poor electrical conductivity and low electrocatalytic activity to advance the development of biosensors.

## 5. Metal-based porous structures

### 5.1 Monometallic-based porous structures

Porous metal-based materials have long been known as good biomaterials and drug carriers<sup>97,98</sup> and have good prospects for application in biological applications and biosensing. In early studies, metallic materials were one of the candidates for metal

implants in the human body due to their sufficient strength and suitable mechanical properties,<sup>99</sup> and other properties, as follows: (1) porous metal has good biocompatibility, stiffness and porosity and (2) porous metal provides open space for the inward growth of bone tissue, thus accelerating the osseointegration process.<sup>100–102</sup> The unique bone-like properties of porous tantalum allow it to be used as a material for large implants, not just as a coating like other porous metals. In addition, porous tantalum also promotes the growth of soft tissues,<sup>103</sup> including the formation of blood vessels, which are found assembled on the surface of porous tantalum and inside the structure.<sup>104</sup> Porous tantalum has a trabecular geometry that can be used to simulate bone tissue, as well as open cell structures (Fig. 7a). The mechanical properties of porous materials significantly depend on their geometric design, including their porosity and unit cell type. The porosity of all types of human bones shows a gradual change from a dense outer cortex to a spongy inner cancellous tissue. Therefore, porous biomaterials must mimic the natural progressive structure of the human skeleton. Li *et al.* demonstrated that porous Fe and Zn with a precisely controlled geometry can be successfully prepared using SLM and possess mechanical properties comparable to that of human bone trabeculae.<sup>105,106</sup> However, although porous nanoparticles significantly increase the available surface area, there is a lack of theoretical understanding



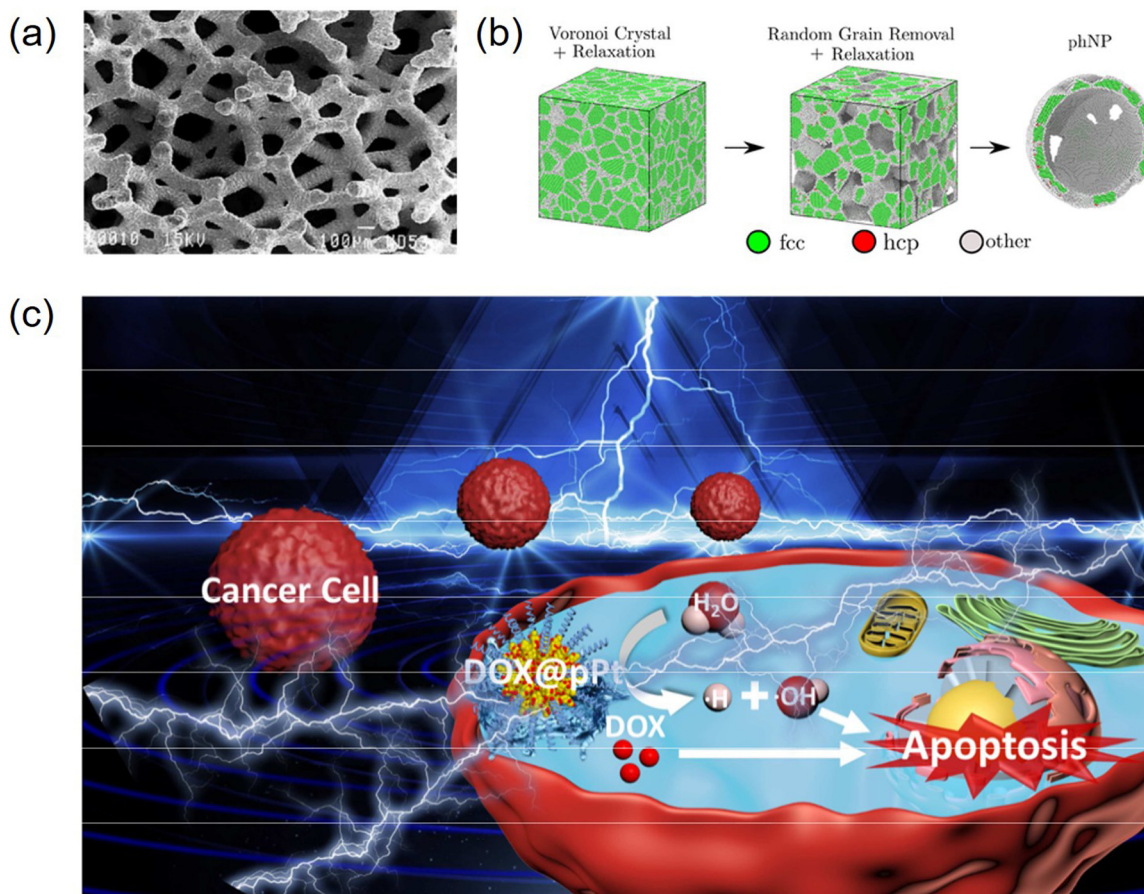


Fig. 7 (a) Structure of porous tantalum. SEM of porous tantalum with small pores and high interconnectivity and porosity. (b) Schematic illustration of thermal stability of hollow porous gold nanoparticles: a molecular dynamics study. (c) Schematic illustration of pPt-based drug delivery system for synergistic electrodynamic/chemotherapy of cancer. Images reprinted with permission from Hacking *et al.* (2000, *J. Biomed. Mater. Res.*), Felipe *et al.* (2020, *JCIM*) and Xu *et al.* (2020, *Biomaterials*), respectively.

and scarce experimental information on how their porosity is controlled or it dominates their stability. As shown in Fig. 7b, Felipe *et al.* used classical molecular dynamics simulations to elucidate the specific characteristics and properties of gold porous hollow nanoparticles and how they differ from nonporous nanoparticles,<sup>107</sup> demonstrating how porosity introduces surface stresses and causes minor transitions in various scenarios with an increase in temperature, improving the stability of porous materials and providing new opportunities for biological applications. In addition, porous metal-based nanomaterials have a wide range of development prospects in drug delivery systems due to their good loading rates and biocompatibility.

Noble metal nanoparticles possess catalytic properties for scavenging reactive oxygen species (ROS) and good biocompatibility, and thus can be used as promising drug delivery platforms for mitigating oxidative stress damage to normal tissues by certain chemotherapeutic drugs. Precious metal materials have inert reactivity *in vivo* and *in vitro*, are biocompatible and have low cytotoxicity.<sup>108</sup> Chen *et al.* used platinum nanoparticles (pPt NPs) with porous structures as anticancer drug delivery carriers to achieve synergistic chemotherapy (Fig. 7c).<sup>109</sup> Using polyethylene glycol (PEG) as a capping layer and the porous

structure of pPt NPs, the obtained pPt-PEG NPs were loaded with the anticancer drug adriamycin (DOX), and this study proposed a new concept of cancer combination therapy with better therapeutic effects. Metal nanoparticles are designed and prepared as a multifunctional platform for the combined treatment of multiple cancers, especially chemophotothermal therapy, due to their excellent optical properties and photothermal conversion.<sup>110,111</sup> Nanocarriers with porous structures have demonstrated potential and possibilities for drug delivery and photothermal therapy.<sup>112</sup> Yang *et al.* constructed porous Au@Pt nanoparticles and explored their performance in mitigating oxidative stress damage and tumor growth inhibition by combined chemophotothermal therapy (Fig. 8a and b), showing that porous Au@Pt nanoparticles are a promising platform for photoacoustic imaging-guided DOX delivery and combined chemophotothermal therapy to reduce oxidative stress.<sup>113</sup> He *et al.* found that porous heterogeneously assembled structures of Au-Ag nanoclusters (NCs) are good drug carriers with high loading performance and biocompatibility for cancer therapy, as shown in Fig. 8c, where the porous structures with high loading performance were formed by the assembly of different metal clusters.<sup>114</sup> The composite structure of different metallic



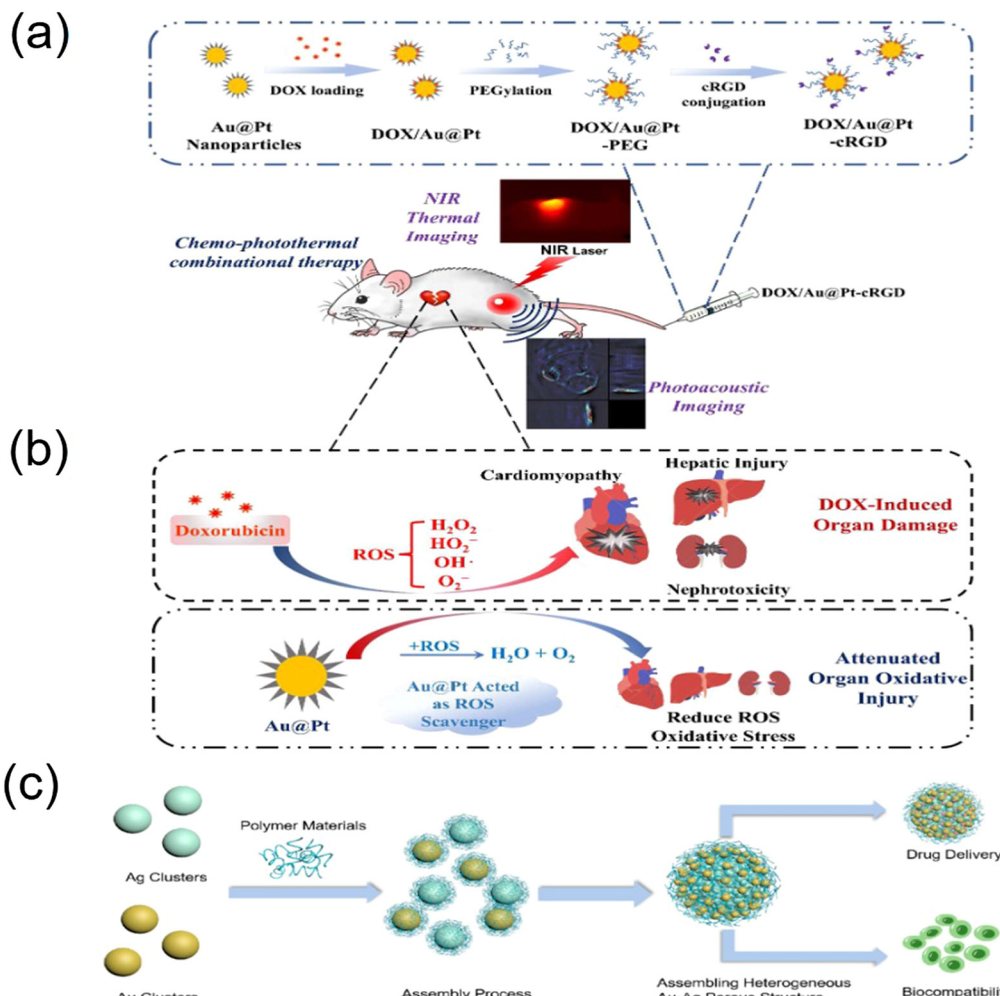


**Fig. 8** Schematic illustration of chemo-photothermal combinational therapy for tumors by multifunctional Au@Pt nanoparticles. (a) Construction of DOX/Au@Pt-cRGD and (b) ROS scavenging property by the catalysis of platinum shell enables the nanostructure to attenuate the DOX-induced organ oxidative injury, especially cardiomyopathy during chemotherapy. The gold core-based nanostructure maintains photoacoustic imaging and high photothermal conversion property, while the surface porous platinum shell not only provides the capability for drug loading but also alleviates the adverse effects of chemodrugs. (c) Schematic diagram of the formation and synthesis of heterogeneous assembly structures of precious metal NCs (Au, Ag). Images reprinted with permission from Yang *et al.* (2018, ACS) and He *et al.* (2022, *IJMS*) respectively.

materials generates new chemical and physical functions that have a wide range of applications in the biological field.<sup>115</sup> In general, porous metal-based structures have good biocompatibility and offer good prospects for biological applications. The Ahmed research team successfully developed an innovative nanomaterial known as the nanostructured mesoporous gold electrode (NMGE). This electrode exhibited exceptionally high sensitivity for the detection of protein phosphorylation through electrochemical signal amplification. By directly adsorbing the BRAF protein, which was purified through immunoprecipitation, on the mesoporous gold electrode, this team successfully bypassed the intricate steps of sensor surface functionalization. This not only streamlined the process but also resulted in a 2.5-fold improvement in sensitivity. Furthermore, there was a significant tenfold enhancement in the detection limit (LOD) compared to previous levels, marking a substantial advancement in this field.<sup>116</sup> Masud and team designed an innovative electrode

known as the mesoporous polystyrene-*block*-polyethylene oxide-gold electrode (MPGE), aimed at creating an ultra-sensitive miRNA detection platform. This electrode was crafted through the utilization of block copolymer micelles (polystyrene-*block*-polyethylene oxide; PS-*b*-PEO), resulting in a uniform porous structure and an augmented functional surface area. Consequently, this approach significantly enhanced the electrocatalytic activity and facilitated the efficient adsorption of a substantial quantity of miRNA.<sup>117</sup> Park and colleagues employed an innovative technique, showcasing its application in microRNA sensors, through the electrochemical assembly of mesoporous gold (Au)-silver (Ag) alloy films. In an electrolyte solution containing spherical polymer micelles, mesoporous gold-silver alloy films with varying molar fractions were electrochemically prepared. Through the adjustment of the composition ratio of Au and Ag ions, precise control of the electrochemically active regions and catalytic activity of the mesoporous bimetallic films was achieved, resulting in

outstanding sensitivity.<sup>118</sup> In general, porous metal-based structures exhibit excellent biocompatibility, offering promising prospects for biological applications. These advancements underscore the potential of these nanomaterials in biomedical applications, paving the way for enhanced diagnostic and therapeutic strategies.

## 5.2 Metal oxide porous structures

Porous metal oxides, including iron oxide, copper oxide, zinc oxide, titanium oxide, zirconium oxide, magnesium oxide, and aluminum oxide, have a wide range of biological and biosensing applications. In recent years, an increasing number of anti-cancer drugs have shown good efficacy in clinical treatment, such as cisplatin, adriamycin (DOX) and paclitaxel, which are widely used in tumor treatment.<sup>119–121</sup> However, there are certain disadvantages associated with the use of these drugs, such as short blood half-lives due to rapid metabolism and elimination by the immune system and non-specific targeting, which can cause damage to normal tissues and cells.<sup>122</sup> In this case, a promising approach to increase the circulation time of anticancer drugs and reduce side effects is the use of suitable drug carriers, which has led to great interest in nanoparticles as drug delivery systems.<sup>123</sup> In addition, porous metal oxides are widely utilized in the field of biosensors because of their good biocompatibility, short response time, high sensitivity and low cost.

**5.2.1 Porous structure of iron oxide.** Iron oxide porous nanoparticles (IOPNP) are promising for biological applications, with the main advantages of simple synthetic route, good biocompatibility, easy modification, maximum signal-active surface, and good dispersion in liquid media.<sup>124,125</sup> Yu *et al.* used polyethylene glycol bisamine ( $\text{NH}_2\text{-PEG-NH}_2$ ) as a spacer to encapsulate folic acid (FA) on the surface of iron oxide porous nanorods (IOPNR) to produce effective targeting agents.<sup>123</sup> As shown in Fig. 9a, the results indicate that iron oxide porous nanorods loaded with DOX could reduce the cardiotoxicity of DOX compared to pure DOX. Wu *et al.* found that porous iron oxide-based

nanorods coated with polyelectrolyte polymers<sup>126</sup> formed nanocapsules, and depending on the denseness of the polyelectrolyte shell layer on the nanorod surface, the permeability of the synthesized nanocapsules could be varied by ionic strength and exhibit stimulus-responsive controlled behavior or slow-release behavior, which could be used as stimulus-responsive controlled carriers or slow-release carriers, respectively. In addition, Gong *et al.* reported a simple method for the preparation of novel HA cross-linked  $\text{Fe}_3\text{O}_4$  nanoparticles ( $\text{Fe}_3\text{O}_4\text{-DOX} + \text{HA}$ ) for DOX delivery (Fig. 9b). The nanoparticles combined the tumor-targeting function of chemotherapy with the tumor-associated macrophage (TAM)-targeting function of M1 polarization.<sup>127</sup> Masud's group constructed gold-supported nanoporous iron oxide nanocubes ( $\text{Au-NPFe}_2\text{O}_3\text{NC}$ ) for the detection of horseradish peroxidase (HRP)-like activity. This inherently autoantibody sensor exhibited excellent detection sensitivity ( $\text{LOD} = 0.08 \text{ U mL}^{-1}$ ) and repeatability (% RSD = <5% for  $n = 3$ ), and the readings of p53-specific autoantibodies could be analyzed using electrochemistry and colorimetry (naked-eye).<sup>128</sup> Islam *et al.* developed an ultra-sensitive and specific electrochemical sensor using the electrocatalytic activity of a novel superparamagnetic nanoparticle graphene oxide-supported iron oxide (GO/IO hybrid material) and the signal enhancement capability of the  $[\text{Ru}(\text{NH}_3)_6]^{3+}/[\text{Fe}(\text{CN})_6]^{3-}$  electrocatalytic cycle. It was used to detect cancer-associated microRNAs (miRNAs). Clinical utility in ovarian cancer cell lines with high sensitivity (10 cells) and good reproducibility (% RSD = <5% for  $n = 3$ ).<sup>129</sup> Bhattacharjee *et al.* reported the synthesis and application of the peroxidase-mimetic activity of mesoporous iron oxide (MIO) for the detection of global DNA methylation in colorectal cancer cell lines. The target DNA was extracted and denatured to obtain ssDNA, followed by its direct adsorption on the surface of a bare screen-printed gold electrode (SPGE). Subsequently, a 5-methylcytosine antibody (5mC)-functionalized nanomaterial (MIO-5mC) was used to recognize the methylcytosine groups present on the SPGE.<sup>130</sup> Boriachek *et al.*

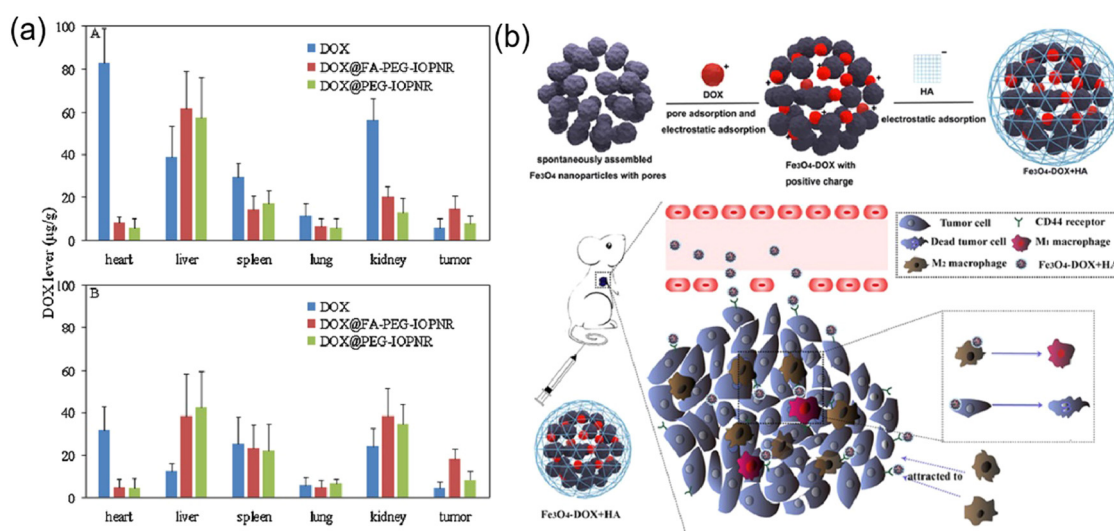


Fig. 9 (a) Biodistribution of free DOX and DOX@modified IOPNR after (A) 4 h and (B) 12 h. (b) Schematic illustration of the preparation and antitumor mechanism. Images reprinted with permission from Yu *et al.* (2014, ELSEVIER) and Gong *et al.* (2019, ELSEVIER), respectively.

described a simple method for the direct isolation and subsequent detection of specific populations of exosomes using an engineered superparamagnetic material with multifunctional properties, namely, gold-loaded iron oxide nanocubes (Au-NPFe<sub>2</sub>O<sub>3</sub>NC). The PLAP-specific exosomes present in placental cell-conditioned media could be visually observed, as well as recognized by ultraviolet-visible and electrochemical detection. This highly sensitive, rapid, and inexpensive assay can be used to quantify specific groups of exosomes for a variety of clinical applications, especially pregnancy complications.<sup>131</sup> The porous structure formed by iron oxide combined with different nanomaterials can be used more effectively as a drug carrier for cancer therapy with good biocompatibility and targeting.

**5.2.2 Porous copper oxides structures.** Copper oxide (CuO) nanoparticles have a controllable particle size of less than 5 nm.<sup>132,133</sup> When self-assembled into nanoclusters, the porous structure leads to a large specific surface area with high Cu content, which increases the active reaction sites and improves the efficiency of Fenton-like reactions.<sup>134,135</sup> As shown in Fig. 10a, CuO nanoclusters (CuO NCs) obtained after the addition of sodium dodecyl sulfate (SDS) surfactant were encapsulated by SiO<sub>2</sub> shells and etched with NaOH solution. Subsequently, they were modified with folic acid (FA) to target cancer cells, and the obtained CuO NCs-FA were delivered to HeLa cells to verify the feasibility of intracellular Fenton-like reactions.<sup>136</sup> In addition, polydopamine-modified CuO combined with natural glucose oxidase (GOD), in which CuO maximizes the cascade catalytic efficiency with a high loading rate (47.1%) due to the elaborate hollow mesoporous structure

(Fig. 10b), was combined with NIR-II-induced thermal effects for combined O<sub>2</sub>-promoted starvation and photothermal-chemical kinetic treatment.<sup>137</sup> In addition, copper oxide (Cu<sub>2</sub>O), as a low-toxic, environmentally friendly p-type semiconductor, has received widespread attention for its application in the fields of photocatalysis, catalysts, adsorption, sensors, etc.<sup>138–140</sup>

Among the developed nanostructures, porous structures are highly desirable because of their high specific surface area, abundant active sites and surface accessibility. Thus far, several synthetic strategies have been successfully developed to prepare porous Cu<sub>2</sub>O crystals, including templating, surfactant-assisted synthesis, electrochemical deposition, and dealloying.<sup>141</sup> For example, as shown in Fig. 10c, Song *et al.* synthesized porous Cu<sub>2</sub>O nanostructures by adjusting the concentration of PVP and the growth solution environment.<sup>142</sup> Yu *et al.* synthesized carbon layer-coated Cu<sub>2</sub>O mesoporous nanorods *via* a facile method of chemical oxidation and subsequent carbonization at 500 °C under N<sub>2</sub>.<sup>143</sup> However, these methods are relatively complex, and thus Zhu *et al.* developed a rapid, simple and economical method for the synthesis of porous nanomaterials by oxidizing urea to CO<sub>2</sub> as a carbon source using sodium hypochlorite as a green oxidant to prepare fine-grained cross-linked Cu precursors (Fig. 10d). These precursors were further reduced by sodium ascorbate to pure Cu<sub>2</sub>O nanospheres (NPs) with a porous morphology at room temperature and found to exhibit high sensitivity and excellent selectivity in the determination of glucose and L-cysteine, making them suitable for the detection of serum samples with reliable results.<sup>144</sup>

**5.2.3 Porous structures of titanium oxide.** The ideal anti-cancer drug delivery system should possess the combination of

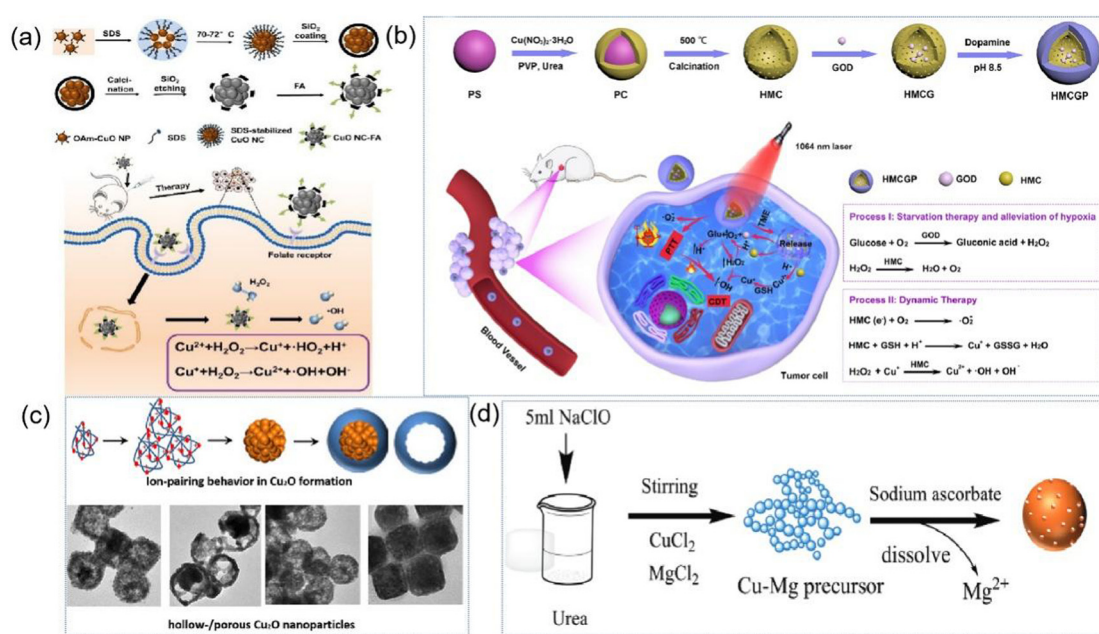


**Fig. 10** (a) Schematic illustration for the synthesis of CuO NCs and CuO NCs-FA, cellular uptake of CuO NCs-FA and intracellular Fenton-like reaction. (b) Schematic illustration of the synthesis of HMCGP and the theranostic mechanism of HMCGP for starvation therapy-promoted alleviation of tumor hypoxia and combined photothermal-catalytic therapy by a cascade enzymatic reaction. (c) Schematic illustration of the synthesis of hollow Cu<sub>2</sub>O nanostructure. (d) Synthetic route of Cu<sub>2</sub>O NPs. Images reprinted with permission from Jin *et al.* (2022, *ACES*), Wang *et al.* (2022, *ACS Appl.*), Song *et al.* (2020, *ACS*) and Zhu *et al.* (2021, *J. Mater. Chem. B*), respectively.



cancer cell-targeting and stimulator-triggered drug release. Porous titanium dioxide ( $\text{TiO}_2$ ) has the potential to satisfy this requirement because of its interesting properties, such as high photocatalytic activity and functional surface.<sup>145</sup> Titanium dioxide is a typical n-type semiconductor material with a wide range of applications including photocatalysis,<sup>146</sup> energy storage and conversion,<sup>147</sup> sun protection<sup>148</sup> and sensor research.<sup>149</sup> Especially in the medical field, it is used as a matrix for anti-cancer agents, implants and stem cell expansion due to its low cost, chemical stability,<sup>150</sup> non-toxicity<sup>151</sup> and good biocompatibility.<sup>152</sup>

Wang *et al.* developed novel polyethyleneimine (PEI)-modified multifunctional porous titanium dioxide nanoparticles.<sup>153</sup> To further achieve targeted delivery, folic acid, as a tumor-targeting agent that effectively promotes specific uptake by tumor cells through receptor-mediated endocytosis, was chemically coupled to the surface of the functionalized porous titanium dioxide nanoparticles by the free amine groups of PEI. Malignancies remain a major health burden worldwide and there is an urgent need for effective treatment strategies. Herein, Yin *et al.* reported the synthesis of upconversion nanoparticles with a mesoporous titanium dioxide ( $\text{mTiO}_2$ ) shell layer for near-infrared (NIR)-triggered drug delivery and synergistic targeting of cancer therapy,<sup>154</sup> which provides another drug-carrying function for anticancer drugs due to the large specific surface area and porous structure of titanium dioxide. The surface-modified hyaluronic acid not only ensures controlled release of the drug, but also endows the system with the ability to target cancer cells.  $\text{TiO}_2$  has good biocompatibility, relatively high electrical conductivity, environmentally friendly properties, and chemical and thermal stability, and is also widely used in protein and immobilized biosensors.<sup>155</sup> The electrochemical properties of titanium dioxide depend not only on its crystal structure but also on its lattice properties (e.g., size, geometry, porosity, and surface area).<sup>156</sup> Thus, to develop high-performance biosensors, efforts have been

made to synthesize titanium dioxide with a controllable morphology and pore structure. Guo *et al.* successfully prepared a freestanding titanium dioxide hollow fiber *via* a simple, scalable electrospun nanofiber membrane-template-assisted sol-gel method and applied it for the immobilization of glucose oxidase (GOD) and biosensing.<sup>157</sup>

**5.2.4 Other metal oxides.** Other metal oxides (alumina, magnesium oxide and zinc oxide) have shown some promise in biological applications and biosensing. Zinc oxide ( $\text{ZnO}$ ) is one of the most representative chemically resistant n-type oxide semiconductor materials. Kim *et al.* prepared porous nanorods and two hierarchical structures of  $\text{ZnO}$  nanostructures consisting of porous nanosheets or crystalline nanorods by reacting oleic acid dissolved ethanol solution and a water-soluble zinc precursor solution in the presence of sodium hydroxide.<sup>158</sup> Fig. 11a shows the pore size, volume distribution and specific surface area of the three  $\text{ZnO}$  nanostructures, all enabling the sensitive and selective detection of  $\text{C}_2\text{H}_5\text{OH}$ . Nanoporous anodic aluminum oxide (NAA) is suitable for optical biosensing because of its transparency in the visible range, photoluminescence<sup>159</sup> and high and tunable surface area/volume ratio. In addition, when produced under appropriate anodic oxidation conditions, its self-ordered structure gives it a photonic resistance band similar to that of photonic crystals. Recently, nano-engineered NAA has also been applied in label-free biosensing applications.<sup>160</sup> Magnesium oxide ( $\text{MgO}$ ) nanoparticles, as important metal oxide nanoparticles, have received significant attention for biomedical applications due to their good biocompatibility and biodegradability.<sup>161</sup> In addition to their significant bactericidal and tumor suppressive effects,<sup>162,163</sup>  $\text{MgO}$  nanoparticles have been used as potential drug candidates,<sup>164</sup> magnetic resonance imaging agents and thermal therapy systems.<sup>162</sup> Considering the different sensitivities of cancer cells and normal cells to lysosomes, Qu *et al.* designed pH-sensitive, biodegradable and imaging-ready porous magnesium oxide nanoparticles ( $\text{MgO}/\text{Eu}$ ) that can support Eu atoms,<sup>165</sup> as shown in

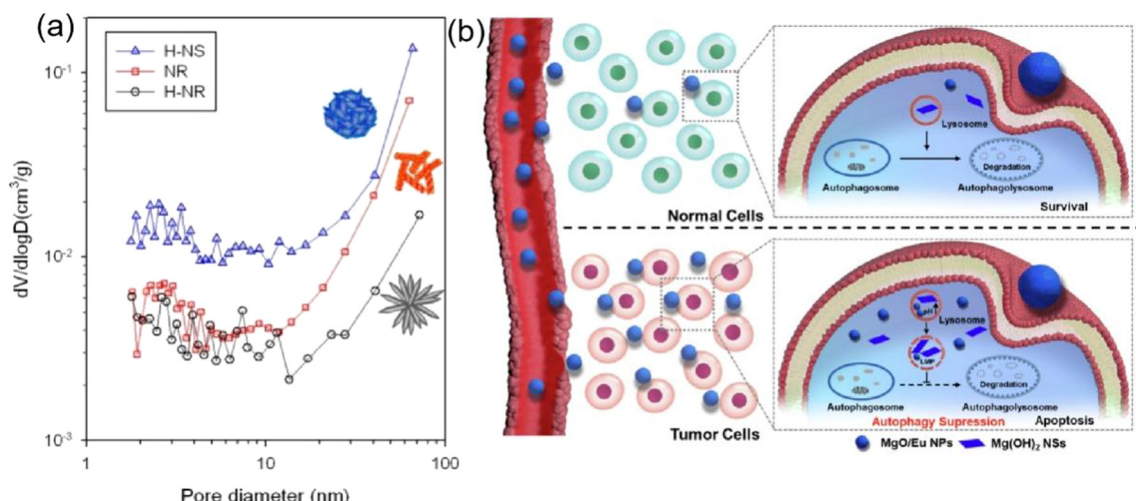


Fig. 11 (a) Pore size distribution of heat-treated H-NS, NR, and H-NR  $\text{ZnO}$  nanostructures determined from nitrogen adsorption–desorption isotherms. (b) Illustration of the role of  $\text{MgO}/\text{Eu}$  NPs as a selective lysosome-autophagy system inhibitor. Images reprinted with permission from Kim *et al.* (2011, Sensors) and Qu *et al.* (2021, ELSEVIER), respectively.

Fig. 11b, which were highly sensitive to  $H^+$ -rich environments, especially in the lysosomes of cancer cells.

## 6. Conclusions

In conclusion, porous nanomaterials demonstrate extensive prospects in the fields of biosensing and *in vivo/in vitro* applications. To date, substantial progress has been achieved in the design and synthesis of porous nanomaterials, involving diverse preparation methods combined with various ligands and materials to attain functional porous structures. However, it is still a challenge to effectively utilize the design of these porous nanomaterials. Through the modification of functional groups in porous nanomaterials, a high loading rate, elevated specific surface area, and excellent biocompatibility have been achieved, enhancing their capabilities in cancer treatment and biosensing applications. These materials hold potential to overcome current obstacles in cancer immunotherapy, thereby improving the anticancer efficacy. Their unique porous structure enables the loading of a substantial amount of immunotherapeutically relevant biomolecules for targeted delivery, modulation of the tumor microenvironment, and regulation of immune cell functions. Their high porosity allows efficient drug loading, guiding them to tumor cells through binding to the targeted fraction on their surface, and ultimately, binding to the cleavable shell. The distinctive structure of porous nanomaterials facilitates highly targeted drug delivery, laying the foundation for personalized cancer treatment. The adjustment of the size and shape of porous structures enables precise treatment of different types of tumors, minimizing damage to healthy tissues. Beyond their application in cancer treatment, the porous structure of nanomaterials can also be employed to regulate immune responses, holding potential value in treating autoimmune diseases or enhancing vaccine effectiveness. These porous nanomaterials exhibit promising results in both *in vitro* and *in vivo* models. The key to their successful application is their biocompatibility, and further in-depth research is needed to explore the response of these materials in different biological systems, ensuring their long-term safety and stability. Additionally, porous nanomaterials have attracted attention in the field of biosensing due to their large specific surface area, high porosity, abundant functional groups, and ease of modification. Coupled with their excellent conductivity, these materials facilitate charge transfer and substance exchange between electrodes and solutions. Biosensors based on porous materials excel in detecting heavy metal ions, small molecules, proteins, and nucleic acids. In summary, porous nanomaterials hold immense potential not only for *in vivo/in vitro* applications and biosensing but also for substance detection in various fields. The interdisciplinary nature of porous nanomaterial research, spanning materials science, biology, chemistry, and more, encourages collaboration and cross-disciplinary research, promising to accelerate the development and innovation in the application of porous nanomaterials. Thus, in the future, through different ligand modifications and

the assembly of diverse materials, the application of porous nanomaterials is anticipated to achieve significant breakthroughs.

## Conflicts of interest

The authors declare no competing financial interest.

## Acknowledgements

This work was supported by the Chongqing Municipal Natural Science Foundation: CSTB2022NSCQ-MSX013; Scientific Foundation Project of Chongqing Education Commission: KJQN20190436; National Natural Science Foundation of China: 81127901, 12074051.

## References

- 1 Z. Luo, S. Fan, C. Gu, W. Liu, J. Chen, B. Li and J. Liu, Metal-Organic Framework (MOF)-based Nanomaterials for Biomedical Applications, *Curr. Med. Chem.*, 2019, **26**, 3341–3369.
- 2 D. Karaman, M. P. Sarparanta, J. M. Rosenholm and A. J. Airaksinen, Multimodality Imaging of Silica and Silicon Materials *In Vivo*, *Adv. Mater.*, 2018, **30**, e1703651.
- 3 H. A. Santos, E. Mäkilä, A. J. Airaksinen, L. M. Bimbo and J. Hirvonen, Porous silicon nanoparticles for nanomedicine: preparation and biomedical applications, *Nanomedicine*, 2014, **9**, 535–554.
- 4 J. Zhou, Y. Li, W. Wang, X. Tan, Z. Lu and H. Han, Metal-organic frameworks-based sensitive electrochemiluminescence biosensing, *Biosens. Bioelectron.*, 2020, **164**, 112332.
- 5 P. Kumar, K.-H. Kim, K. Vellingiri, P. Samaddar, P. Kumar, A. Deep and N. Kumar, Hybrid porous thin films: Opportunities and challenges for sensing applications, *Biosens. Bioelectron.*, 2018, **104**, 120–137.
- 6 J. Ferre-Borrull, J. Pallares, G. Macias and L. F. Marsal, Nanostructural Engineering of Nanoporous Anodic Alumina for Biosensing Applications, *Materials*, 2014, **7**, 5225–5253.
- 7 V. Stojanovic, F. Cunin, J. O. Durand, M. Garcia and M. Gary-Bobo, Potential of porous silicon nanoparticles as an emerging platform for cancer theranostics, *J. Mater. Chem. B*, 2016, **4**, 7050–7059.
- 8 Y. Park, J. Yoo, M. H. Kang, W. Kwon and J. Joo, Photoluminescent and biodegradable porous silicon nanoparticles for biomedical imaging, *J. Mater. Chem. B*, 2019, **7**, 6271–6292.
- 9 G. Hong, A. L. Antaris and H. Dai, Near-infrared fluorophores for biomedical imaging, *Nat. Biomed. Eng.*, 2017, **1**, 0010–0031.
- 10 H. C. Zhou, J. R. Long and O. M. Yaghi, Introduction to metal–organic frameworks, *Chem. Rev.*, 2012, **112**, 673–674.
- 11 A. S. Cheung and D. J. Mooney, Engineered Materials for Cancer Immunotherapy, *Nano Today*, 2015, **10**, 511–531.
- 12 C. T. t Hagan, Y. B. Medik and A. Z. Wang, Nanotechnology Approaches to Improving Cancer Immunotherapy, *Adv. Cancer Res.*, 2018, **139**, 35–56.



13 G. Chong, J. Zang, Y. Han, R. Su, N. Weeranoppanant, H. Dong and Y. Li, Bioengineering of nano metal-organic frameworks for cancer immunotherapy, *Nano Res.*, 2021, **14**, 1244–1259.

14 F. Boateng and W. Ngwa, Delivery of Nanoparticle-Based Radiosensitizers for Radiotherapy Applications, *Int. J. Mol. Sci.*, 2020, **21**, 273–294.

15 N. Thakur, S. Thakur, S. Chatterjee, J. Das and P. C. Sil, Nanoparticles as Smart Carriers for Enhanced Cancer Immunotherapy, *Front. Chem.*, 2020, **8**, 597806.

16 C. Xu, C. Lei and C. Yu, Mesoporous Silica Nanoparticles for Protein Protection and Delivery, *Front. Chem.*, 2019, **7**, 290.

17 C. Xu, C. Lei, Y. Wang and C. Yu, Dendritic Mesoporous Nanoparticles: Structure, Synthesis and Properties, *Angew. Chem., Int. Ed.*, 2022, **61**, e202112752.

18 I. Mikelez-Alonso, A. Aires and A. L. Cortajarena, Cancer Nano-Immunotherapy from the Injection to the Target: The Role of Protein Corona, *Int. J. Mol. Sci.*, 2020, **21**, 519–535.

19 K. Lu, T. Aung, N. Guo, R. Weichselbaum and W. Lin, Nanoscale Metal–Organic Frameworks for Therapeutic, Imaging, and Sensing Applications, *Adv. Mater.*, 2018, **30**, e1707634.

20 A. Cao, Z. Ye, Y. Yang, Y. Liu, H. Wang and Y. Liu, Fluorescent protein-based multi-functional nanoparticles for bioimaging and drug delivery, *Nanomedicine*, 2016, **12**, 455.

21 J. Joo, X. Liu, V. R. Kotamraju, E. Ruoslahti, Y. Nam and M. J. Sailor, Gated Luminescence Imaging of Silicon Nanoparticles, *ACS Nano*, 2015, **9**, 6233–6241.

22 C. Martínez-Boubeta, L. Balcells, R. Cristófol, C. Sanfeliu, E. Rodríguez, R. Weissleder, S. Lope-Piedrafita, K. Simeonidis, M. Angelakeris, F. Sandiumenge, A. Calleja, L. Casas, C. Monty and B. Martínez, Self-assembled multifunctional Fe/MgO nanospheres for magnetic resonance imaging and hyperthermia, *Nanomedicine*, 2010, **6**, 362–370.

23 C. A. Marquette and L. J. Blum, State of the art and recent advances in immunoanalytical systems, *Biosens. Bioelectron.*, 2006, **21**, 1424–1433.

24 S. Dhanekar and S. Jain, Porous silicon biosensor: Current status, *Biosens. Bioelectron.*, 2013, **41**, 54–64.

25 A. D. Kartashova, K. A. Gonchar, D. A. Chermoshentsev, E. A. Alekseeva, M. B. Gongalsky, I. V. Bozhev, A. A. Eliseev, S. A. Dyakov, J. V. Samsonova and L. A. Osminkina, Surface-Enhanced Raman Scattering-Active Gold-Decorated Silicon Nanowire Substrates for Label-Free Detection of Bilirubin, *ACS Biomater. Sci. Eng.*, 2022, **8**, 4175–4184.

26 K. Tian, Y. S. Ma, Y. K. Liu, M. H. Wang and M. Du, Hierarchically structured hollow bimetallic ZnNi MOF microspheres as a sensing platform for adenosine detection, *Sens. Actuators, B*, 2019, **303**, 127199.

27 D. F. Thomas, Porous silicon, *Handbook of Nanostructured Materials and Nanotechnology*, 2000.

28 L. M. Bimbo, M. Sarparanta, H. A. Santos, A. J. Airaksinen, E. Makila, T. Laaksonen, L. Peltonen, V. P. Lehto, J. Hirvonen and J. Salonen, Biocompatibility of thermally hydrocarbonized porous silicon nanoparticles and their biodistribution in rats, *ACS Nano*, 2010, **4**, 3023–3032.

29 D. X. Zhang, L. Esser, R. B. Vasani, H. Thissen and N. H. Voelcker, Porous silicon nanomaterials: recent advances in surface engineering for controlled drug-delivery applications, *Nanomedicine*, 2019, **14**, 3213–3230.

30 H. A. Santos, E. Makila, A. J. Airaksinen, L. M. Bimbo and J. Hirvonen, Porous silicon nanoparticles for nanomedicine: preparation and biomedical applications, *Nanomedicine*, 2014, **9**, 535–554.

31 J. Salonen, L. Laitinen, A. M. Kaukonen, J. Tuura, M. Bjorkqvist, T. Heikkila, K. Vaha-Heikkila, J. Hirvonen and V. P. Lehto, Mesoporous silicon microparticles for oral drug delivery: loading and release of five model drugs, *J. Controlled Release*, 2005, **108**, 362–374.

32 E. Blanco, A. Hsiao, G. U. Ruiz-Esparza, M. G. Landry, F. Meric-Bernstam and M. Ferrari, Molecular-targeted nanotherapies in cancer: enabling treatment specificity, *Mol. Oncol.*, 2011, **5**, 492–503.

33 P. A. Kulyavtsev and R. P. Spencer, Drug delivery via porous silicon: a focused patent review, *Pharm. Pat. Anal.*, 2017, **6**, 77–85.

34 M. Jeong, Y. Jung, J. Yoon, J. Kang, S. H. Lee, W. Back, H. Kim, M. J. Sailor, D. Kim and J. H. Park, Porous Silicon-Based Nanomedicine for Simultaneous Management of Joint Inflammation and Bone Erosion in Rheumatoid Arthritis, *ACS Nano*, 2022, **16**, 16118–16132.

35 K. Trzeciak, A. Chotera-Ouda, S. Bak, II and M. J. Potrzebowski, Mesoporous Silica Particles as Drug Delivery Systems-The State of the Art in Loading Methods and the Recent Progress in Analytical Techniques for Monitoring These Processes, *Pharmaceutics*, 2021, **13**, 14230–14240.

36 M. Zhang, J.-J. Ye, Y. Xia, Z.-Y. Wang, C.-X. Li, X.-S. Wang, W. Yu, W. Song, J. Feng and X.-Z. Zhang, Platelet-Mimicking Biotaxis Targeting Vasculature-Disrupted Tumors for Cascade Amplification of Hypoxia-Sensitive Therapy, *ACS Nano*, 2019, **13**, 14230–14240.

37 Rita Elena Serda, US8926994, 2015.

38 Michael J. Sailor, US9394369, 2016.

39 B. Kim, Q. Yang, L. W. Chan, S. N. Bhatia, E. Ruoslahti and M. J. Sailor, Fusogenic porous silicon nanoparticles as a broad-spectrum immunotherapy against bacterial infections, *Nanoscale Horiz.*, 2021, **6**, 330–340.

40 J. Pellico, P. J. Gawne and R. T. M. de Rosales, Radiolabeling of nanomaterials for medical imaging and therapy, *Chem. Soc. Rev.*, 2021, **50**, 3355–3423.

41 C. Yao, P. Wang, X. Li, X. Hu, J. Hou, L. Wang and F. Zhang, Near-Infrared-Triggered Azobenzene-Liposome/Upconversion Nanoparticle Hybrid Vesicles for Remotely Controlled Drug Delivery to Overcome Cancer Multidrug Resistance, *Adv. Mater.*, 2016, **28**, 9341–9348.

42 T. van der Geest, P. Laverman, J. M. Metselaar, G. Storm and O. C. Boerman, Radionuclide imaging of liposomal drug delivery, *Expert Opin. Drug Delivery*, 2016, **13**, 1231–1242.

43 T. Nakamura, F. Sugihara, H. Matsushita, Y. Yoshioka, S. Mizukami and K. Kikuchi, Mesoporous silica



nanoparticles for <sup>(19)F</sup> magnetic resonance imaging, fluorescence imaging, and drug delivery, *Chem. Sci.*, 2015, **6**, 1986–1990.

44 J. H. Park, L. Gu, G. von Maltzahn, E. Ruoslahti, S. N. Bhatia and M. J. Sailor, Biodegradable luminescent porous silicon nanoparticles for *in vivo* applications, *Nat. Mater.*, 2009, **8**, 331–336.

45 O. Syshchyk, V. A. Skryshevsky, O. O. Soldatkin and A. P. Soldatkin, Enzyme biosensor systems based on porous silicon photoluminescence for detection of glucose, urea and heavy metals, *Biosens. Bioelectron.*, 2015, **66**, 89–94.

46 S. Zhang, M. Sun, X. Wang, J. Wang, Z. Jia, X. Lv and X. Huang, Spectral-Free Double Light Detection of DNA Based on a Porous Silicon Bragg Mirror, *Sensors*, 2021, **11**, 27–41.

47 R. Vercauteren, A. Leprince, J. Mahillon and L. A. Francis, Porous Silicon Biosensor for the Detection of Bacteria through Their Lysate, *Biosensors*, 2021, **21**, 8248–8257.

48 R. Layouni, T. Cao, M. B. Coppock, P. E. Laibinis and S. M. Weiss, Peptide-Based Capture of Chikungunya Virus E2 Protein Using Porous Silicon Biosensor, *Nature*, 2021, **21**, 8248.

49 O. M. Yaghi, G. Li and H. Li, Selective binding and removal of guests in a microporous metal–organic framework, *Nature*, 1995, **378**, 703–706.

50 W. P. Lustig, S. Mukherjee, N. D. Rudd, A. V. Desai, J. Li and S. K. Ghosh, Metal–organic frameworks: functional luminescent and photonic materials for sensing applications, *Chem. Soc. Rev.*, 2017, **46**, 3242–3285.

51 P. Horcajada, C. Serre, M. Vallet-Regí, M. Sebban, F. Taulelle and G. Férey, Metal–organic frameworks as efficient materials for drug delivery, *Angew. Chem., Int. Ed.*, 2006, **45**, 5974–5978.

52 J. W. Zhang, H. T. Zhang, Z. Y. Du, X. Wang, S. H. Yu and H. L. Jiang, Water-stable metal–organic frameworks with intrinsic peroxidase-like catalytic activity as a colorimetric biosensing platform, *Chem. Commun.*, 2014, **50**, 1092–1094.

53 L. Ai, L. Li, C. Zhang, J. Fu and J. Jiang, MIL-53(Fe): a metal–organic framework with intrinsic peroxidase-like catalytic activity for colorimetric biosensing, *Chemistry*, 2013, **19**, 15105–15108.

54 G. H. Qiu, W. Z. Lu, P. P. Hu, Z. H. Jiang, L. P. Bai, T. R. Wang, M. M. Li and J. X. Chen, A metal–organic framework based PCR-free biosensor for the detection of gastric cancer associated microRNAs, *J. Inorg. Biochem.*, 2017, **177**, 138–142.

55 P. Horcajada, R. Gref, T. Baati, P. K. Allan, G. Maurin, P. Couvreur, G. Férey, R. E. Morris and C. Serre, Metal–organic frameworks in biomedicine, *Chem. Rev.*, 2012, **112**, 1232–1268.

56 C. He, K. Lu and W. Lin, Nanoscale metal–organic frameworks for real-time intracellular pH sensing in live cells, *J. Am. Chem. Soc.*, 2014, **136**, 12253–12256.

57 R. Xu, Y. Wang, X. Duan, K. Lu, D. Micheroni, A. Hu and W. Lin, Nanoscale Metal–Organic Frameworks for Ratiometric Oxygen Sensing in Live Cells, *J. Am. Chem. Soc.*, 2016, **138**, 2158–2161.

58 Y. Lu, B. Yan and J. L. Liu, Nanoscale metal–organic frameworks as highly sensitive luminescent sensors for  $\text{Fe}^{2+}$  in aqueous solution and living cells, *Chem. Commun.*, 2014, **50**, 9969–9972.

59 J. Zhao, Y. N. Wang, W. W. Dong, Y. P. Wu, D. S. Li and Q. C. Zhang, A Robust Luminescent  $\text{Tb}^{(III)}$ -MOF with Lewis Basic Pyridyl Sites for the Highly Sensitive Detection of Metal Ions and Small Molecules, *Inorg. Chem.*, 2016, **55**, 3265–3271.

60 W. Ma, Q. Jiang, P. Yu, L. Yang and L. Mao, Zeolitic imidazolate framework-based electrochemical biosensor for *in vivo* electrochemical measurements, *Anal. Chem.*, 2013, **85**, 7550–7557.

61 Y. Cui, H. Xu, Y. Yue, Z. Guo, J. Yu, Z. Chen, J. Gao, Y. Yang, G. Qian and B. Chen, A luminescent mixed-lanthanide metal–organic framework thermometer, *J. Am. Chem. Soc.*, 2012, **134**, 3979–3982.

62 D. Zhao, D. Yue, K. Jiang, L. Zhang, C. Li and G. Qian, Isostructural  $\text{Tb}^{(3+)}/\text{Eu}^{(3+)}$  Co-Doped Metal–Organic Framework Based on Pyridine-Containing Dicarboxylate Ligands for Ratiometric Luminescence Temperature Sensing, *Inorg. Chem.*, 2019, **58**, 2637–2644.

63 Q. Hu, N. Kong, Y. Chai, Z. Xing, Y. Wu, J. Zhang, F. Li and X. Zhu, A lanthanide nanocomposite with cross-relaxation enhanced near-infrared emissions as a ratiometric nanothermometer, *Nanoscale Horiz.*, 2022, **7**, 1177–1185.

64 S. Keskin and S. Kizilel, Biomedical Applications of Metal Organic Frameworks, *Ind. Eng. Chem. Res.*, 2011, **50**, 1799–1812.

65 D. Yang, G. Yang, S. Gai, F. He, G. An, Y. Dai, R. Lv and P. Yang, Au25 cluster functionalized metal–organic nanostructures for magnetically targeted photodynamic/photothermal therapy triggered by single wavelength 808 nm near-infrared light, *Nanoscale*, 2015, **7**, 19568–19578.

66 W. Wang, L. Wang, Z. Li and Z. Xie, BODIPY-containing nanoscale metal–organic frameworks for photodynamic therapy, *Chem. Commun.*, 2016, **52**, 5402–5405.

67 C. He, K. Lu, D. Liu and W. Lin, Nanoscale metal–organic frameworks for the co-delivery of cisplatin and pooled siRNAs to enhance therapeutic efficacy in drug-resistant ovarian cancer cells, *J. Am. Chem. Soc.*, 2014, **136**, 5181–5184.

68 A. R. Chowdhuri, D. Laha, S. Pal, P. Karmakar and S. K. Sahu, One-pot synthesis of folic acid encapsulated upconversion nanoscale metal organic frameworks for targeting, imaging and pH responsive drug release, *Dalton Trans.*, 2016, **45**, 18120–18132.

69 Q. Xiao, Y. Liu, Y. Zhong and W. Zhu, A citrate sol–gel method to synthesize  $\text{Li}_2\text{ZrO}_3$  nanocrystals with improved  $\text{CO}_2$  capture properties, *J. Mater. Chem.*, 2011, **21**, 3838–3842.

70 Y. A. Li, X. D. Zhao, H. P. Yin, G. J. Chen, S. Yang and Y. B. Dong, A drug-loaded nanoscale metal–organic framework with a tumor targeting agent for highly effective hepatoma therapy, *Chem. Commun.*, 2016, **52**, 14113–14116.



71 M. Tavakolizadeh, M. Atarod, S. J. Seyyed Tabaei, S. Sojdeh, E. Nazarzadeh Zare, M. Rabiee and N. Rabiee, Green modified-UiO-66/MXene sandwich composites for gene-chemotherapy synergistic cancer suppression: Co-delivery of doxorubicin and pCRISPR, *Alexandria Eng. J.*, 2023, **80**, 144–154.

72 K. M. Au, A. Satterlee, Y. Min, X. Tian, Y. S. Kim, J. M. Caster, L. Zhang, T. Zhang, L. Huang and A. Z. Wang, Folate-targeted pH-responsive calcium zole-dronate nanoscale metal–organic frameworks: Turning a bone antiresorptive agent into an anticancer therapeutic, *Biomaterials*, 2016, **82**, 178–193.

73 W. Lin, Q. Hu, J. Yu, K. Jiang, Y. Yang, S. Xiang, Y. Cui, Y. Yang, Z. Wang and G. Qian, Low Cytotoxic Metal–Organic Frameworks as Temperature-Responsive Drug Carriers, *ChemPlusChem*, 2016, **81**, 804–810.

74 J. Della Rocca, D. Liu and W. Lin, Nanoscale Metal–Organic Frameworks for Biomedical Imaging and Drug Delivery, *Acc. Chem. Res.*, 2011, **44**, 957–968.

75 W. Hatakeyama, T. J. Sanchez, M. D. Rowe, N. J. Serkova, M. W. Liberatore and S. G. Boyes, Synthesis of gadolinium nanoscale metal–organic framework with hydrotripes: manipulation of particle size and magnetic resonance imaging capability, *ACS Appl. Mater. Interfaces*, 2011, **3**, 1502–1510.

76 K. M. Taylor-Pashow, J. Della Rocca, Z. Xie, S. Tran and W. Lin, Postsynthetic modifications of iron-carboxylate nanoscale metal–organic frameworks for imaging and drug delivery, *J. Am. Chem. Soc.*, 2009, **131**, 14261–14263.

77 T. Zhang, L. Wang, C. Ma, W. Wang, J. Ding, S. Liu, X. Zhang and Z. Xie, BODIPY-containing nanoscale metal–organic frameworks as contrast agents for computed tomography, *J. Mater. Chem. B*, 2017, **5**, 2330–2336.

78 J. Wu, F. Xu, S. Li, P. Ma, X. Zhang, Q. Liu, R. Fu and D. Wu, Porous Polymers as Multifunctional Material Platforms toward Task-Specific Applications, *Adv. Mater.*, 2019, **31**, e1802922.

79 P. Stroeve and N. Iler, Biotechnical and other applications of nanoporous membranes, *Trends Biotechnol.*, 2011, **29**, 259–266.

80 P. Guo, J. Huang, Y. Zhao, C. R. Martin, R. N. Zare and M. A. Moses, Nanomaterial Preparation by Extrusion through Nanoporous Membranes, *Small*, 2018, **14**, e1703493.

81 A. Shiohara, B. Prieto-Simon and N. H. Voelcker, Porous polymeric membranes: fabrication techniques and biomedical applications, *J. Mater. Chem. B*, 2021, **9**, 2129–2154.

82 D. Wu, F. Xu, B. Sun, R. Fu, H. He and K. Matyjaszewski, Design and preparation of porous polymers, *Chem. Rev.*, 2012, **112**, 3959–4015.

83 N. Oku, Innovations in Liposomal DDS Technology and Its Application for the Treatment of Various Diseases, *Biol. Pharm. Bull.*, 2017, **40**, 119–127.

84 S. Y. Yang, J.-A. Yang, E.-S. Kim, G. Jeon, E. J. Oh, K. Y. Choi, S. K. Hahn and J. K. Kim, Single-file diffusion of protein drugs through cylindrical nanochannels, *ACS Nano*, 2010, **4**, 3817–3822.

85 G. I. Benic and C. H. F. Hämmeler, Horizontal bone augmentation by means of guided bone regeneration, *Periodontology 2000*, 2014, **66**, 13–40.

86 D. Rothamel, F. Schwarz, M. Sager, M. Herten, A. Sculean and J. Becker, Biodegradation of differently cross-linked collagen membranes: an experimental study in the rat, *Clin. Oral Implants Res.*, 2005, **16**, 369–378.

87 A. Klinger, R. Asad, L. Shapira and Y. Zubery, *In vivo* degradation of collagen barrier membranes exposed to the oral cavity, *Clin. Oral Implants Res.*, 2010, **21**, 873–876.

88 L. M. Delgado, Y. Bayon, A. Pandit and D. I. Zeugolis, To cross-link or not to cross-link? Cross-linking associated foreign body response of collagen-based devices, *Tissue Eng., Part B*, 2015, **21**, 298–313.

89 S. M. Reddy, *Materials for Chemical Sensing*, 2017, ch. 4, pp. 75–103, DOI: [10.1007/978-3-319-47835-7\\_4](https://doi.org/10.1007/978-3-319-47835-7_4).

90 L. Movileanu, Watching single proteins using engineered nanopores, *Protein Pept. Lett.*, 2014, **21**, 235–246.

91 J. Mota, N. Yu, S. G. Caridade, G. M. Luz, M. E. Gomes, R. L. Reis, J. A. Jansen, X. F. Walboomers and J. F. Mano, Chitosan/bioactive glass nanoparticle composite membranes for periodontal regeneration, *Acta Biomater.*, 2012, **8**, 4173–4180.

92 M. Herten, R. E. Jung, D. Ferrari, D. Rothamel, V. Golubovic, A. Molenberg, C. H. F. Hämmeler, J. Becker and F. Schwarz, Biodegradation of different synthetic hydrogels made of polyethylene glycol hydrogel/RGD-peptide modifications: an immunohistochemical study in rats, *Clin. Oral Implants Res.*, 2009, **20**, 116–125.

93 S. H. Park, D. S. Park, J. W. Shin, Y. G. Kang, H. K. Kim, T. R. Yoon and J.-W. Shin, Scaffolds for bone tissue engineering fabricated from two different materials by the rapid prototyping technique: PCL versus PLGA, *J. Mater. Sci.: Mater. Med.*, 2012, **23**, 2671–2678.

94 A. de la Escosura-Muñiz and A. Merkoçi, A nanochannel/nanoparticle-based filtering and sensing platform for direct detection of a cancer biomarker in blood, *Small*, 2011, **7**, 675–682.

95 A. de la Escosura-Muñiz and A. Merkoçi, Nanoparticle based enhancement of electrochemical DNA hybridization signal using nanoporous electrodes, *Chem. Commun.*, 2010, **46**, 9007–9009.

96 I. Sadeghi, J. Kronenberg and A. Asatekin, Selective Transport through Membranes with Charged Nanochannels Formed by Scalable Self-Assembly of Random Copolymer Micelles, *ACS Nano*, 2022, **20**, 277–295.

97 S. R. Li, F. Y. Huo, H. Q. Wang, J. Wang, C. Xu, B. Liu and L. L. Bu, Recent advances in porous nanomaterials-based drug delivery systems for cancer immunotherapy, *J. Nanobiotechnol.*, 2022, **20**, 277.

98 A. Baeza, D. Ruiz-Molina and M. Vallet-Regi, Recent advances in porous nanoparticles for drug delivery in antitumoral applications: inorganic nanoparticles and nanoscale metal–organic frameworks, *Expert Opin. Drug Delivery*, 2017, **14**, 783–796.

99 Y. Li, H. Jahr, J. Zhou and A. A. Zadpoor, Additively manufactured biodegradable porous metals, *Acta Biomater.*, 2020, **115**, 29–50.



100 M. Chimutengwende-Gordon, R. Dowling, C. Pendegrass and G. Blunn, Determining the porous structure for optimal soft-tissue ingrowth: An *in vivo* histological study, *PLoS One*, 2018, **13**, e0206228.

101 Y. Qin, A. Liu, H. Guo, Y. Shen, P. Wen, H. Lin, D. Xia, M. Voshage, Y. Tian and Y. Zheng, Additive manufacturing of Zn-Mg alloy porous scaffolds with enhanced osseointegration: *In vitro* and *in vivo* studies, *Acta Biomater.*, 2022, **145**, 403–415.

102 C. Zhang, L. Zhang, L. Liu, L. Lv, L. Gao, N. Liu, X. Wang and J. Ye, Mechanical behavior of a titanium alloy scaffold mimicking trabecular structure, *J. Orthop. Surg. Res.*, 2020, **15**, 40.

103 G. Mohandas, N. Oskolkov, M. T. McMahon, P. Walczak and M. Janowski, Porous tantalum and tantalum oxide nanoparticles for regenerative medicine, *Acta Neurobiol. Exp.*, 2014, **74**, 188–196.

104 V. K. Balla, S. Bodhak, S. Bose and A. Bandyopadhyay, Porous tantalum structures for bone implants: fabrication, mechanical and *in vitro* biological properties, *Acta Biomater.*, 2010, **6**, 3349–3359.

105 Y. Li, H. Jahr, P. Pavanram, F. S. L. Bobbert, U. Paggi, X. Y. Zhang, B. Pouran, M. A. Leeflang, H. Weinans, J. Zhou and A. A. Zadpoor, Additively manufactured functionally graded biodegradable porous iron, *Acta Biomater.*, 2019, **96**, 646–661.

106 Y. Li, P. Pavanram, J. Zhou, K. Lietaert, F. S. L. Bobbert, Y. Kubo, M. A. Leeflang, H. Jahr and A. A. Zadpoor, Additively manufactured functionally graded biodegradable porous zinc, *Biomater. Sci.*, 2020, **8**, 2404–2419.

107 F. J. Valencia, M. Ramirez, A. Varas, J. Rogan and M. Kiwi, Thermal Stability of Hollow Porous Gold Nanoparticles: A Molecular Dynamics Study, *J. Chem. Inf. Model.*, 2020, **60**, 6204–6210.

108 P. V. Asharani, Y. Lianwu, Z. Gong and S. Valiyaveettil, Comparison of the toxicity of silver, gold and platinum nanoparticles in developing zebrafish embryos, *Nanotoxicology*, 2011, **5**, 43–54.

109 T. Chen, T. Gu, L. Cheng, X. Li, G. Han and Z. Liu, Porous Pt nanoparticles loaded with doxorubicin to enable synergistic Chemo-/Electrodynamic Therapy, *Biomaterials*, 2020, **255**, 120202.

110 N. Zhang, D. Zhu, F. Li, H. Hua, X. Tian and Y. Zhao, Low Density Lipoprotein Peptide-Conjugated Gold Nanorods for Combating Gastric Cancer, *J. Biomed. Nanotechnol.*, 2017, **13**, 134–143.

111 Y. Liu, J. R. Ashton, E. J. Moding, H. Yuan, J. K. Register, A. M. Fales, J. Choi, M. J. Whitley, X. Zhao, Y. Qi, Y. Ma, G. Vaidyanathan, M. R. Zalutsky, D. G. Kirsch, C. T. Badea and T. Vo-Dinh, A Plasmonic Gold Nanostar Theranostic Probe for *In Vivo* Tumor Imaging and Photothermal Therapy, *Theranostics*, 2015, **5**, 946–960.

112 F. Tang, L. Li and D. Chen, Mesoporous silica nanoparticles: synthesis, biocompatibility and drug delivery, *Adv. Mater.*, 2012, **24**, 1504–1534.

113 Q. Yang, J. Peng, Y. Xiao, W. Li, L. Tan, X. Xu and Z. Qian, Porous Au@Pt Nanoparticles: Therapeutic Platform for Tumor Chemo-Photothermal Co-Therapy and Alleviating Doxorubicin-Induced Oxidative Damage, *ACS Appl. Mater. Interfaces*, 2018, **10**, 150–164.

114 X. He, X. Ma, Y. Yang, X. Hu, T. Wang, S. Chen and X. Mao, Metal Cluster Triggered-Assembling Heterogeneous Au-Ag Nanoclusters with Highly Loading Performance and Biocompatible Capability, *Int. J. Mol. Sci.*, 2022, **23**, 11197–11212.

115 S. A. Khan, R. Kanchanapally, Z. Fan, L. Beqa, A. K. Singh, D. Senapati and P. C. Ray, A gold nanocage-CNT hybrid for targeted imaging and photothermal destruction of cancer cells, *Chem. Commun.*, 2012, **48**, 6711–6713.

116 E. Ahmed, M. K. Masud, M. S. A. Hossain, J. Na, A. A. Sina, Y. Yamauchi and M. Trau, Nanostructured mesoporous gold electrodes detect protein phosphorylation in cancer with electrochemical signal amplification, *Analyst*, 2020, **145**, 6639–6648.

117 M. K. Masud, J. Na, T. E. Lin, V. Malgras, A. Preet, A. A. Ibn Sina, K. Wood, M. Billah, J. Kim, J. You, K. Kani, A. E. Whitten, C. Salomon, N. T. Nguyen, M. J. A. Shiddiky, M. Trau, M. S. A. Hossain and Y. Yamauchi, Nanostructured mesoporous gold biosensor for microRNA detection at attomolar level, *Biosens. Bioelectron.*, 2020, **168**, 112429.

118 H. Park, M. K. Masud, J. Na, H. Lim, H. P. Phan, Y. V. Kaneti, A. A. Alothman, C. Salomon, N. T. Nguyen, M. S. A. Hossain and Y. Yamauchi, Mesoporous gold–silver alloy films towards amplification-free ultra-sensitive microRNA detection, *J. Mater. Chem. B*, 2020, **8**, 9512–9523.

119 M. Xie, H. Shi, Z. Li, H. Shen, K. Ma, B. Li, S. Shen and Y. Jin, A multifunctional mesoporous silica nanocomposite for targeted delivery, controlled release of doxorubicin and bioimaging, *Colloids Surf., B*, 2013, **110**, 138–147.

120 Z.-S. Chen, R. W. Robey, M. G. Belinsky, I. Shchaveleva, X.-Q. Ren, Y. Sugimoto, D. D. Ross, S. E. Bates and G. D. Kruh, Transport of methotrexate, methotrexate polyglutamates, and 17beta-estradiol 17-(beta-D-glucuronide) by ABCG2: effects of acquired mutations at R482 on methotrexate transport, *Cancer Res.*, 2003, **63**, 4048–4054.

121 F. P. Seib and D. L. Kaplan, Doxorubicin-loaded silk films: drug-silk interactions and *in vivo* performance in human orthotopic breast cancer, *Biomaterials*, 2012, **33**, 8442–8450.

122 Y. Wu, E. K. Shih, A. Ramanathan, S. Vasudevan and T. Weil, Nano-sized albumin-copolymer micelles for efficient doxorubicin delivery, *Biointerphases*, 2012, **7**, 5.

123 L. Sandiford, A. Phinikaridou, A. Protti, L. K. Meszaros, X. Cui, Y. Yan, G. Frodsham, P. A. Williamson, N. Gaddum, R. M. Botnar, P. J. Blower, M. A. Green and R. T. M. de Rosales, Bisphosphonate-anchored PEGylation and radiolabeling of superparamagnetic iron oxide: long-circulating nanoparticles for *in vivo* multimodal (T1 MRI-SPECT) imaging, *ACS Nano*, 2013, **7**, 500–512.

124 M. J. Jeon, A. C. Gordon, A. C. Larson, J. W. Chung, Y. I. Kim and D. H. Kim, Transcatheter intra-arterial infusion of doxorubicin loaded porous magnetic nanoclusters with iodinated oil for the treatment of liver cancer, *Biomaterials*, 2016, **88**, 25–33.

125 W. Zhao, Z. Huang, L. Liu, W. Wang, J. Leng and Y. Liu, Porous bone tissue scaffold concept based on shape



memory PLA/Fe<sub>3</sub>O<sub>4</sub>, *Compos. Sci. Technol.*, 2021, **203**, 108563–108604.

126 P. C. Wu, W. S. Wang, Y. T. Huang, H. S. Sheu, Y. W. Lo, T. L. Tsai, D. B. Shieh and C. S. Yeh, Porous iron oxide based nanorods developed as delivery nanocapsules, *Chemistry*, 2007, **13**, 3878–3885.

127 T. Gong, X. Song, L. Yang, T. Chen, T. Zhao, T. Zheng, X. Sun, T. Gong and Z. Zhang, Spontaneously formed porous structure and M(1) polarization effect of Fe(3)O(4) nanoparticles for enhanced antitumor therapy, *Int. J. Pharm.*, 2019, **559**, 329–340.

128 M. K. Masud, S. Yadav, M. N. Islam, N. T. Nguyen, C. Salomon, R. Kline, H. R. Alamri, Z. A. Alothman, Y. Yamauchi, M. S. A. Hossain and M. J. A. Shiddiky, Gold-Loaded Nanoporous Ferric Oxide Nanocubes with Peroxidase-Mimicking Activity for Electrocatalytic and Colorimetric Detection of Autoantibody, *Anal. Chem.*, 2017, **89**, 11005–11013.

129 S. Balaban Hanoglu, D. Harmanci, N. Ucar, S. Evran and S. Timur, Recent Approaches in Magnetic Nanoparticle-Based Biosensors of miRNA Detection, *Magnetochemistry*, 2023, **9**, 23.

130 R. Bhattacharjee, S. Tanaka, S. Moriam, M. K. Masud, J. Lin, S. M. Alshehri, T. Ahamad, R. R. Salunkhe, N. T. Nguyen, Y. Yamauchi, M. S. A. Hossain and M. J. A. Shiddiky, Porous nanozymes: the peroxidase-mimetic activity of mesoporous iron oxide for the colorimetric and electrochemical detection of global DNA methylation, *J. Mater. Chem. B*, 2018, **6**, 4783–4791.

131 K. Boriachek, M. K. Masud, C. Palma, H. P. Phan, Y. Yamauchi, M. S. A. Hossain, N. T. Nguyen, C. Salomon and M. J. A. Shiddiky, Avoiding Pre-Isolation Step in Exosome Analysis: Direct Isolation and Sensitive Detection of Exosomes Using Gold-Loaded Nanoporous Ferric Oxide Nanozymes, *Anal. Chem.*, 2019, **91**, 3827–3834.

132 F. Bai, D. Wang, Z. Huo, W. Chen, L. Liu, X. Liang, C. Chen, X. Wang, Q. Peng and Y. Li, A versatile bottom-up assembly approach to colloidal spheres from nanocrystals, *Angew. Chem., Int. Ed.*, 2007, **46**, 6650–6653.

133 Z. Lu, M. Ye, N. Li, W. Zhong and Y. Yin, Self-assembled TiO<sub>2</sub> nanocrystal clusters for selective enrichment of intact phosphorylated proteins, *Angew. Chem., Int. Ed.*, 2010, **49**, 1862–1866.

134 Y. Gao, F. Yang, Q. Yu, R. Fan, M. Yang, S. Rao, Q. Lan, Z. Yang and Z. Yang, Three-dimensional porous Cu@Cu(2)O aerogels for direct voltammetric sensing of glucose, *Mikrochim. Acta*, 2019, **186**, 192.

135 Y.-Y. Li, P. Kang, S.-Q. Wang, Z.-G. Liu, Y.-X. Li and Z. Guo, Ag nanoparticles anchored onto porous CuO nanobelts for the ultrasensitive electrochemical detection of dopamine in human serum, *Sens. Actuators, B*, 2021, **327**, 12887–12896.

136 X. Jin, H. Zhao, Z. Chao, X. Wang, Q. Zhang, H. Ju and Y. Liu, Self-assembled Cupric Oxide Nanoclusters for Highly efficient chemodynamic therapy, *Chem. – Asian J.*, 2022, **17**, e202200296.

137 J. Wang, J. Ye, W. Lv, S. Liu, Z. Zhang, J. Xu, M. Xu, C. Zhao, P. Yang and Y. Fu, Biomimetic Nanoarchitectonics of Hollow Mesoporous Copper Oxide-Based Nanozymes with Cascade Catalytic Reaction for Near Infrared-II Reinforced Photothermal-Catalytic Therapy, *ACS Appl. Mater. Interfaces*, 2022, **14**, 40645–40658.

138 P. Ling, Q. Zhang, T. Cao and F. Gao, Versatile Three-Dimensional Porous Cu@Cu(2)O Aerogel Networks as Electrocatalysts and Mimicking Peroxidases, *Angew. Chem., Int. Ed.*, 2018, **57**, 6819–6824.

139 L. Feng, C. Zhang, G. Gao and D. Cui, Facile synthesis of hollow Cu<sub>2</sub>O octahedral and spherical nanocrystals and their morphology-dependent photocatalytic properties, *Nanoscale Res. Lett.*, 2012, **7**, 276.

140 S. Sun and Z. Yang, Cu<sub>2</sub>O-templated strategy for synthesis of definable hollow architectures, *Chem. Commun.*, 2014, **50**, 7403–7415.

141 Z. Qi and J. Weissmüller, Hierarchical nested-network nanostructure by dealloying, *ACS Nano*, 2013, **7**, 5948–5954.

142 X. Song, W. Xu, D. Su, J. Tang and X. Liu, The Synthesis of Hollow/Porous CuO Nanoparticles by Ion-Pairing Behavior Control, *ACS Omega*, 2020, **5**, 1879–1886.

143 L. Yu, G. Li, X. Zhang, X. Ba, G. Shi, Y. Li, P. K. Wong, J. C. Yu and Y. Yu, Enhanced Activity and Stability of Carbon-Decorated Cuprous Oxide Mesoporous Nanorods for CO<sub>2</sub> Reduction in Artificial Photosynthesis, *ACS Catal.*, 2016, **6**, 6444–6454.

144 Y. Zhu, Z. Zhang, X. Song and Y. Bu, A facile strategy for synthesis of porous Cu(2)O nanospheres and application as nanozymes in colorimetric biosensing, *J. Mater. Chem. B*, 2021, **9**, 3533–3543.

145 T.-Y. Tsai, S.-J. Chang, T.-J. Hsueh, H.-T. Hsueh, W.-Y. Weng, C.-L. Hsu and B.-T. Dai, p-Cu<sub>2</sub>O-shell/n-TiO<sub>2</sub>-nanowire-core heterostucture photodiodes, *Nanoscale Res. Lett.*, 2011, **6**, 575.

146 E. Martínez-Ferrero, Y. Sakatani, C. Boissière, D. Gross, A. Fuertes, J. Fraxedas and C. Sanchez, Nanostructured Titanium Oxynitride Porous Thin Films as Efficient Visible-Active Photocatalysts, *Adv. Funct. Mater.*, 2007, **17**, 3348–3354.

147 Y.-G. Guo, J.-S. Hu and L.-J. Wan, Nanostructured Materials for Electrochemical Energy Conversion and Storage Devices, *Adv. Mater.*, 2008, **20**, 2878–2887.

148 A. Jaroenworaluck, W. Sunsaneeyametha, N. Kosachan and R. Stevens, Characteristics of silica-coated TiO<sub>2</sub> and its UV absorption for sunscreen cosmetic applications, *Surf. Interface Anal.*, 2006, **38**, 473–477.

149 Q. Zheng, B. Zhou, J. Bai, L. Li, Z. Jin, J. Zhang, J. Li, Y. Liu, W. Cai and X. Zhu, Self-Organized TiO<sub>2</sub> Nanotube Array Sensor for the Determination of Chemical Oxygen Demand, *Adv. Mater.*, 2008, **20**, 1044–1049.

150 J. Xu, Y. Sun, J. Huang, C. Chen, G. Liu, Y. Jiang, Y. Zhao and Z. Jiang, Photokilling cancer cells using highly cell-specific antibody-TiO(2) bioconjugates and electroporation, *Bioelectrochemistry*, 2007, **71**, 217–222.



151 M. Geetha, A. K. Singh, R. Asokamani and A. K. Gogia, Ti based biomaterials, the ultimate choice for orthopaedic implants – A review, *Prog. Mater. Sci.*, 2009, **54**, 397–425.

152 M. Belicchi, S. Erratico, P. Razini, M. Meregalli, A. Cattaneo, E. Jacchetti, A. Farini, C. Villa, N. Bresolin, L. Porretti, C. Lenardi, P. Milani and Y. Torrente, *Ex vivo* expansion of human circulating myogenic progenitors on cluster-assembled nanostructured TiO<sub>2</sub>, *Biomaterials*, 2010, **31**, 5385–5396.

153 T. Wang, H. Jiang, L. Wan, Q. Zhao, T. Jiang, B. Wang and S. Wang, Potential application of functional porous TiO<sub>2</sub> nanoparticles in light-controlled drug release and targeted drug delivery, *Acta Biomater.*, 2015, **13**, 354–363.

154 M. Yin, E. Ju, Z. Chen, Z. Li, J. Ren and X. Qu, Upconverting nanoparticles with a mesoporous TiO<sub>2</sub>(2) shell for near-infrared-triggered drug delivery and synergistic targeted cancer therapy, *Chemistry*, 2014, **20**, 14012–14017.

155 P. Si, S. Ding, J. Yuan, X. W. D. Lou and D.-H. Kim, Hierarchically structured one-dimensional TiO<sub>2</sub> for protein immobilization, direct electrochemistry, and mediator-free glucose sensing, *ACS Nano*, 2011, **5**, 7617–7626.

156 G. K. Mor, K. Shankar, M. Paulose, O. K. Varghese and C. A. Grimes, Enhanced photocleavage of water using titania nanotube arrays, *Nano Lett.*, 2005, **5**, 191–195.

157 Q. Guo, L. Liu, M. Zhang, H. Hou, Y. Song, H. Wang, B. Zhong and L. Wang, Hierarchically mesostructured porous TiO<sub>2</sub>(2) hollow nanofibers for high performance glucose biosensing, *Biosens. Bioelectron.*, 2017, **92**, 654–660.

158 K. M. Kim, H. R. Kim, K. I. Choi, H. J. Kim and J. H. Lee, Design of highly sensitive C<sub>2</sub>H<sub>5</sub>OH sensors using self-assembled ZnO nanostructures, *Sensors*, 2011, **11**, 9685–9699.

159 A. Santos, V. S. Balderrama, M. Alba, P. Formentín, J. Ferré-Borrull, J. Pallarès and L. F. Marsal, Tunable Fabry–Pérot interferometer based on nanoporous anodic alumina for optical biosensing purposes, *Nanoscale Res. Lett.*, 2012, **7**, 370.

160 A. Santos, T. Kumeria and D. Losic, Optically optimized photoluminescent and interferometric biosensors based on nanoporous anodic alumina: a comparison, *Anal. Chem.*, 2013, **85**, 7904–7911.

161 B. Mangalampalli, N. Dumala and P. Grover, Acute oral toxicity study of magnesium oxide nanoparticles and microparticles in female albino Wistar rats, *Regul. Toxicol. Pharmacol.*, 2017, **90**, 170–184.

162 C. Martínez-Boubeta, L. Balcells, R. Cristòfol, C. Sanfelix, E. Rodríguez, R. Weissleder, S. Lope-Piedrafita, K. Simeonidis, M. Angelakeris, F. Sandiumenge, A. Calleja, L. Casas, C. Monty and B. Martínez, Self-assembled multi-functional Fe/MgO nanospheres for magnetic resonance imaging and hyperthermia, *Nanomedicine*, 2010, **6**, 362–370.

163 D.-R. Di, Z.-Z. He, Z.-Q. Sun and J. Liu, A new nanocryosurgical modality for tumor treatment using biodegradable MgO nanoparticles, *Nanomedicine*, 2012, **8**, 1233–1241.

164 S. Shen, P. S. Chow, F. Chen and R. B. H. Tan, Submicron particles of SBA-15 modified with MgO as carriers for controlled drug delivery, *Chem. Pharm. Bull.*, 2007, **55**, 985–991.

165 X. Qu, Z. Liu, N. Li, B. Ma, H. Zhao, Y. Li, B. Lei and Y. Du, Biodegradable biocompatible MgO/Eu nanodrug with Acid–Base conversion capacity for targeted lung cancer therapy, *Chem. Eng. J.*, 2022, **446**, 136323–136333.

